AFRL-RY-WP-TR-2012-0257

PROBE ARRAY CORRECTION WITH STRONG TARGET INTERACTIONS

John Schindler

ARCON Corporation

AUGUST 2012
Interim Report

Approved for public release; distribution unlimited.

See additional restrictions described on inside pages

STINFO COPY

AIR FORCE RESEARCH LABORATORY
SENSORS DIRECTORATE
WRIGHT-PATTERSON AIR FORCE BASE, OH 45433-7320
AIR FORCE MATERIEL COMMAND
UNITED STATES AIR FORCE

NOTICE AND SIGNATURE PAGE

Using Government drawings, specifications, or other data included in this document for any purpose other than Government procurement does not in any way obligate the U.S. Government. The fact that the Government formulated or supplied the drawings, specifications, or other data does not license the holder or any other person or corporation; or convey any rights or permission to manufacture, use, or sell any patented invention that may relate to them.

This report was cleared for public release by the USAF 88th Air Base Wing (88 ABW) Public Affairs Office (PAO) and is available to the general public, including foreign nationals.

Copies may be obtained from the Defense Technical Information Center (DTIC) (http://www.dtic.mil).

AFRL-RY-WP-TR-2012-0257 HAS BEEN REVIEWED AND IS APPROVED FOR PUBLICATION IN ACCORDANCE WITH THE ASSIGNED DISTRIBUTION STATEMENT.

*//signature//	//signature//
KRISTOPHER T. KIM, Work Unit Manager Antenna Technology Branch Electromagnetics Technology Division	DAVID D. CURTIS, Chief Antenna Technology Branch Electromagnetics Technology Division

This report is published in the interest of scientific and technical information exchange, and its publication does not constitute the Government's approval or disapproval of its ideas or findings.

*Disseminated copies will show "//signature//" stamped or typed above the signature blocks.

REPORT DOCUMENTATION PAGE

Form Approved
OMB No. 0704-0188

The public reporting burden for this collection of information is estimated to average 1 hour per response, including the time for reviewing instructions, searching existing data sources, gathering and maintaining the data needed, and completing and reviewing the collection of information. Send comments regarding this burden estimate or any other aspect of this collection of information, including suggestions for reducing this burden, to Department of Defense, Washington Headquarters Services, Directorate for Information Operations and Reports (0704-0188), 1215 Jefferson Davis Highway, Suite 1204, Arlington, VA 22202-4302. Respondents should be aware that notwithstanding any other provision of law, no person shall be subject to any penalty for failing to comply with a collection of information if it does not display a currently valid OMB control number. **PLEASE DO NOT RETURN YOUR FORM TO THE ABOVE ADDRESS**.

1. REPORT DATE *(DD-MM-YY)*	2. REPORT TYPE	3. DATES COVERED *(From - To)*
August 2012	Interim	01 May 2011 – 31 May 2012

4. TITLE AND SUBTITLE
PROBE ARRAY CORRECTION WITH STRONG TARGET INTERACTIONS

5a. CONTRACT NUMBER
IN-HOUSE

5b. GRANT NUMBER

5c. PROGRAM ELEMENT NUMBER
61102F

6. AUTHOR(S)
John Schindler (ARCON Corporation)

5d. PROJECT NUMBER
2307

5e. TASK NUMBER
HE

5f. WORK UNIT NUMBER
Y04N

7. PERFORMING ORGANIZATION NAME(S) AND ADDRESS(ES)

Electromagnetics Technology Division
Antenna Technology Branch (AFRL/RYHA)
Sensors Directorate, Air Force Research Laboratory
Wright-Patterson Air Force Base, OH 45433-7320
Air Force Materiel Command, United States Air Force

ARCON Corporation
260 Bear Hill Road
Waltham, MA 02451

8. PERFORMING ORGANIZATION REPORT NUMBER
AFRL-RY-WP-TR-2012-0257

9. SPONSORING/MONITORING AGENCY NAME(S) AND ADDRESS(ES)

Air Force Research Laboratory
Sensors Directorate
Wright-Patterson Air Force Base, OH 45433-7320
Air Force Materiel Command
United States Air Force

10. SPONSORING/MONITORING AGENCY ACRONYM(S)
AFRL/RYHA

11. SPONSORING/MONITORING AGENCY REPORT NUMBER(S)
AFRL-RY-WP-TR-2012-0257

12. DISTRIBUTION/AVAILABILITY STATEMENT
Approved for public release; distribution unlimited.

13. SUPPLEMENTARY NOTES
PAO Case Number: 88ABW-2012-4564, cleared 24 August 2012. Report contains color.

14. ABSTRACT

We analyze technical problems associated with using an array of probes to measure simultaneously the near fields scattered by a target to decrease collection times. Array-target coupling distorts the fields to be measured. Element mutual coupling modifies measurements. To minimize coupling, active loading at array elements with strong target interaction is analyzed numerically. Loading minimizes perturbations in the target currents. There is little advantage to using in-situ mutual impedances to determine loads. We provide a probe array compensation theory based on the Lorentz reciprocity theorem giving the open circuit probe array voltages. Voltage corrections are developed from array calibration and measurements of the incident plane wave. Numerical study shows that (a) corrections to the measured voltages due to the presence of the array are small and (b) corrections due to the other elements of the array can be important but corrected with calibration. Errors introduced by the use of realizable calibration sources and loads and experimental errors are estimated. Results of this study suggest a hybrid measurement process.

-- See following page for alternate abstract. --

15. SUBJECT TERMS
electromagnetic near field measurements, bistatic scattering cross section, array mutual impedances, Lorentz reciprocity theorem

16. SECURITY CLASSIFICATION OF:			17. LIMITATION OF ABSTRACT:	18. NUMBER OF PAGES	19a. NAME OF RESPONSIBLE PERSON (Monitor)
a. REPORT	b. ABSTRACT	c. THIS PAGE			Kristopher T. Kim
Unclassified	Unclassified	Unclassified	SAR	50	19b. TELEPHONE NUMBER *(Include Area Code)* N/A

14. ABSTRACT, concluded

We analyze technical problems associated with the use of an array of probes to measure simultaneously the near fields scattered by a target. The measurements are made with the objective of estimating the far zone bistatic scattering from the target using established electromagnetic signal processing techniques. An array of probes is proposed to speed the collection of required near field samples. However, the array increases the potential for electromagnetic coupling between the array and the target, thereby distorting the fields to be measured. Further, mutual coupling between array elements in the presence of the scattering body may change the near field measured at each probe array element when compared to that measured by an isolated probe.

To minimize the array-target coupling, we propose that the array employ active loading at each array element to minimize currents on the array elements. Proper active loading requires knowledge of the mutual impedances between array elements, which, in general, depend on the location and orientation of the array with respect to the scattering target. To assess the requirement for measurements of in-situ mutual impedances, we consider a probe array with strong interaction between the target and the array. We investigate the perturbations on the plane wave induced currents on a target consisting of a plate due to the presence of the loaded, five element dipole probe array. Numerical results found using NEC4 indicate that active loading of the probe array is required to minimize the perturbations in the target currents. However, we find in this case that there is little advantage to using in-situ mutual impedances in place of free space impedances in determining the active loads.

Also, we provide a probe array compensation theory based on the Lorentz reciprocity theorem. The theory permits expression of the open circuit probe array voltages in terms of (1) the required surface integral involving the near fields scattered by the target and the near fields radiated by the probe array with no target-array interaction, and (2) correction voltages due to the presence of the other array elements and target-array interactions. The correction voltages are of two types. One type is due to perturbations in the target scattered field due to the presence of the probe array and is unknown and not available for compensation of the measured voltage at the probe array. Another type of correction voltage is associated with plane wave induced currents on the probe array when located in free space. These correction voltages can be developed as part of the probe array calibration and measurements of the incident plane wave. A numerical study of the flat plate-probe array configuration indicates that (a) corrections to the measured probe array voltages due to perturbations in the scattered field from the presence of the probe array are small, even when cancellation of the probe array currents is determined using the free space mutual impedances of the array, and (b) corrections due to the presence of the other elements of the probe array can be important, but the corrections can be determined in terms of the free space current distributions on the array as part of the array calibration process. Also, errors in the probe array voltage measurements are introduced by the use of realizable sources in the probe array during calibration and realizable loads during scattering measurements. When the array is calibrated in free space and used to cancel the array currents during near field measurements, errors in the open circuit voltages can be large for array elements that are close to the target under test. Experimental errors in achieving probe array current cancellation cause errors in the voltage measurements that can be significant as well.

These conclusions are potentially significant since they seem to indicate that free space mutual impedances of the probe array are sufficient for the simultaneous measurement with small error of near scattered field samples so long as elements of the probe array are not too close to the target under test. These results suggest a hybrid measurement process. For probe array locations and orientations with respect to the target where there is likely to be large coupling, in-situ mutual impedances would be required, slowing the measurement process. When little coupling is anticipated, the free space mutual impedances of the array can be used, thereby speeding the measurement process. These conclusions are based on a limited numerical investigation of one probe array structure and target configuration. Suggestions for further study are provided.

Contents

Approved for public release; distribution unlimited.

List of Figures

Approved for public release; distribution unlimited.

Approved for public release; distribution unlimited.

List of Tables

Approved for public release; distribution unlimited.

1 Summary

The measurement of bistatic radar cross sections of large vehicles with far field techniques is time consuming, expensive and requires physically large and less secure measurement facilities. Alternatively, near field scattering measurements permit estimation of bistatic scattering using smaller and more secure facilities. Advanced electromagnetic signal processing enables the transformation of the multiple, near field measurements to the required complete set of far field bistatic cross sections. Still, near field measurements are time consuming and therefore expensive. The objective of this work is to investigate the feasibility of significantly reducing the time to make near field scattering measurements through the use of an array of near field probes instead of the conventional single probe. However, the use of an array of near field probes introduces technical problems. Coupling between the physically larger probe array and the scattering body may introduce errors in the near field measurements. Also, mutual coupling between the probe array elements in the presence of the scattering body may change the near field measured at each probe array element from that measured by an isolated probe.

In this work, we analyze these technical problems and describe an approach to compensate for the errors introduced by the use of the probe array. Previously, [SCH] we studied an active loading approach to minimize the electromagnetic interactions between an array of field probes and a nearby scattering body. The loading minimizes the currents on the array of field probes while simultaneously measuring the open circuit voltages induced in the probes. Numerical studies of simple examples showed that the currents on the approximately half wavelength probe array elements are canceled effectively only at the single load point, leaving residual currents to reradiate and modify the plane wave induced currents on the scattering body. Nevertheless, examination of the currents on surrogate target dipoles indicates that substantial reductions in the errors in the induced currents results from the single point loading of each element in a three element probe array. Results of this work revealed the need to study requirements for (a) in-situ mutual impedance measurements of the probe array at each sample position with respect to the target to minimize the probe array currents, (b) compensation of the open circuit, plane wave induced probe array voltages, and (c) experimental and numerical confirmation of the active loading approach. In this report, we examine study topics (a) and (b).

To evaluate the need for in-situ mutual impedance measurements, we consider a probe array with strong interaction between the target and the array. Specifically, we consider a surrogate flat plate with a five element dipole probe array located near the plate and in the direction of the specular, plane wave induced scattering from the plate. To minimize perturbations in the plane wave induced currents on the target due to coupling between the target and the array, currents on the probe array are minimized using active loading at the feeds of the array elements. Proper active loading requires that we measure the mutual impedances between elements of the probe array, ideally when the array is in the presence of the target. However, such in-situ measurements would have to be made at each array location and orientation with respect to the target, slowing the overall measurement process. Alternatively, the mutual impedances could be measured in free space, with the target absent, speeding the measurement process. However, use of these free space mutual impedances will result in imperfect probe element current cancellation and may result in increased perturbation of the plane wave induced currents on the target.

Approved for public release; distribution unlimited.

We investigate the perturbations of the plane wave induced currents on the plate due to the presence of the loaded, five element dipole probe array using NEC4. Results indicate that active loading of the probe array is required to minimize the perturbations in the target currents. However, we find in this case that there is little advantage to using in-situ mutual impedances in determining the active loads. If this result is generalized, it could be significant in reducing the time required for near field measurements since the probe array mutual impedances need not be measured at each probe array position and orientation with respect to the scattering body. Instead, the probe array mutual impedances need be measured only once when the probe array is in free space and these mutual impedances can be used to determine the active loads on the array for all positions of the array with respect to the scattering body.

However, this is not the complete story. The coupling between the array and the target under test can introduce errors in the measured voltages at the probe array elements. These errors are due to (a) the assumption that there is no target-array coupling in interpreting the measurements, (b) calibration of the probe array in free space where there is no interaction with the target and (c) failure to achieve adequate current cancellation in the probe array elements during measurements of the open circuit voltages at the array elements. To understand these additional sources of error, we provide a probe array compensation theory based on the Lorentz reciprocity theorem. The theory permits expression of the open circuit probe array voltages in terms of (a) the required surface integral involving the near fields scattered by the target and the near fields radiated by the probe array with no target-array interaction and (b) correction voltages due to the presence of the array elements and the target-array interactions. The correction voltages are of two types. One type is due to perturbations in the target scattered field because of the presence of the probe array. This correction voltage is unknown and not available for compensation of the measured voltage at the probe array. Another type of correction voltage is associated with plane wave induced currents on the probe array when located in free space. These correction voltages can be developed as part of the probe array calibration and measurements of the incident plane wave. A numerical study of the surrogate flat plate-probe array configuration indicates that (a) corrections to the measured probe array voltages due to perturbations in the scattered field from the presence of the probe array are small, even when cancellation of the probe array currents is determined using the free space mutual impedances of the array, and (b) corrections due to the presence of the other elements of the probe array can be important but the corrections can be determined in terms of the free space current distributions on the array as part of the array calibration process.

Also, errors in the probe array voltage measurements are introduced by the use of realizable sources in the probe array during calibration and realizable loads during scattering measurements. When the array is calibrated in free space and used to cancel the array currents during near field measurements, errors in the open circuit voltages can be large for array elements that are close to the target under test. Experimental errors in achieving probe array current cancellation cause errors in the voltage measurements that can be significant as well.

These results seem to indicate that free space mutual impedances of the probe array are sufficient for the simultaneous measurement of near scattered field samples with small error so long as elements of the array are not too close to the target under test. The effective use of free space mutual impedances obviates the need for in-situ impedance measurements at each location and orientation of the probe array with respect to the scattering body which would slow the overall measurement process. It would seem that a hybrid measurement process should be considered.

Approved for public release; distribution unlimited.

For probe array locations and orientations with respect to the target where there is likely to be large coupling, in-situ mutual impedances would be required, slowing the measurement process. When little coupling is anticipated, the free space mutual impedances of the array can be used, thereby speeding the measurement process. These conclusions are based on a limited numerical investigation of one probe array structure and target configuration. Suggestions for further study are included.

2 Introduction

In previous work [SCH] we studied an approach to reduce the time required for near field scattering measurements by using an array of near field probes to replace the single probe that is conventionally used. However, coupling between the probe array and the scattering body may introduce errors in the near field measurements by perturbing the plane wave induced currents on the body. Further, mutual coupling between the probe array elements in the presence of the scattering body may change the near field measured at each probe array element from that measured by an isolated probe.

Based on an impedance model for the interactions between the probe array and the scattering body, we developed expressions for the measured voltages at each of the transmission line feeds to the probe array elements in terms of (1) the open circuit voltages induced by the plane wave excited body at each probe array element and (2) the in-situ mutual impedances of the probe array. The expressions showed a linear set of relations between the measured voltages and the open circuit voltages as would be expected by the superposition principle. The linear set of equations can be inverted to yield the open circuit, plane wave induced voltages at each probe array element. We hypothesized that these probe element voltages, when corrected for the direct plane wave excitation, are related to the required near field measurements. We also described a separate set of vector network analyzer measurements to yield the in-situ mutual impedances (the mutual impedances in the presence of the scattering body) that are required to invert the measurement equations.

Simple examples of the importance of the open circuit conditions in the measurement of near fields with a dipole probe array were given. Example results were based on a method of moments solution to the electromagnetic interaction problem using NEC4. The open circuit conditions for the half wavelength dipole elements of the probe array minimized the dominant currents on the elements leaving smaller, residual currents on the remaining quarter wavelength sections of the dipoles. Minimization of the dominant currents in the probe array elements reduced the errors in the target dipole currents by more than 20 dB when compared to the free space induced currents.

Minimizing the probe array-target interactions required measurement of the in-situ mutual impedances of the probe array. In general these measurements would be required for each location and orientation of the probe array with respect to the scattering target. However, repeated in-situ impedance measurements will slow the overall measurement process and degrade the promised range efficiency of the probe array.

Approved for public release; distribution unlimited.

In this note we evaluate the feasibility of using the free space mutual impedances of the array in place of the in-situ impedances to derive the open circuit voltages and minimize the array-target interactions. The free space impedances would be measured only once, thereby increasing the efficiency of the overall measurement process. We investigate the feasibility of using free space mutual impedances using an example problem where there is strong interaction between the probe array and the target. This example problem consists of a surrogate flat plate with a five element dipole probe array located near the target and in the specular scattering direction from the target. The effect of using the free space mutual impedances of the probes array in an attempt to create open circuit probe array voltages will be compared to the case when in-situ mutual impedances are used. Errors in the plane wave induced current distributions on the target caused by the probe array will be compared when the probe array currents are canceled using in-situ and free space mutual impedances.

We develop a theory for compensation of the measured voltages in the probe array using the Lorentz reciprocity theorem. The theory relates the measured voltage in each element of the probe array to (a) a surface integral involving the near scattered field from the target and the near radiated fields from the array with no target-array interaction and (b) correction voltages due to the presence of the other array elements and electromagnetic interaction between the array and the scattering body. The correction voltages are expressed in terms of the reaction of the perturbed scattered and incident fields with the currents on the array elements when located in free space. A numerical study of the surrogate flat plate-probe array configuration quantifies the relative importance of the array-target interactions and the array element mutual coupling. In addition, we develop expressions for the errors in the measured voltages due to imperfect calibration of the probe array and imperfect cancellation of the probe array currents.

In this report, Section 3 describes the basic measurement model used to study array-target interactions numerically. The model consists of a surrogate flat plate with a five element dipole probe array located near the target and in the specular scattering direction from the target. This model should provide strong target-array interactions and provide a severe test of the necessity for minimizing these interactions by cancellation of the probe array currents. Section 4 provides results of a numerical analysis of the measurement model using NEC4. Probe array currents are canceled using numerical measurements of the mutual impedances of the probe array with the target absent (free space impedances) and with the target present (in-situ impedances). Currents on the array elements and the flat plate target are compared using active loading cancellation found with the use of both sets of mutual impedances.

In Section 5 we turn to the issue of probe compensation with the objective of quantifying the relationship between the open circuit probe array element voltages as samples of the surface integral involving the near scattered field from the target and the near radiated fields from the array. Since the processing of conventional near field measurements with probes assumes no interaction between the probe and the target or antenna under test, we extend the probe compensation theory developed here to (a) include this assumption and (b) evaluate the effects of this assumption. We provide numerical results using NEC4 for the measurement model described in Section 3 to quantify corrections in the measured probe array voltages due to target-array interactions and the presence of other probe array elements. In addition, we extend the probe compensation theory to assess the errors in the measured voltages due to imperfect calibration of the probe array and imperfect cancellation of the probe array currents at the element terminals.

Approved for public release; distribution unlimited.

3 Measurement Model

We consider a target that interacts strongly with the probe array. The model is shown in Figure 1. It consists of a flat plate of dimensions 2λ by $\lambda/2$ at a distance of 2λ from a 5 element probe array. Here λ denotes the wavelength of the plane wave excitation. As indicated, the measurement array consists of 5 dipoles which are 0.48λ in length with $\lambda/2$ inter-element spacing located on the y axis. The plate and plane wave excitation are oriented so the the probe array is in the far field specular scattering direction from the plate, although the probe array itself is in the near field of the plate scattering.

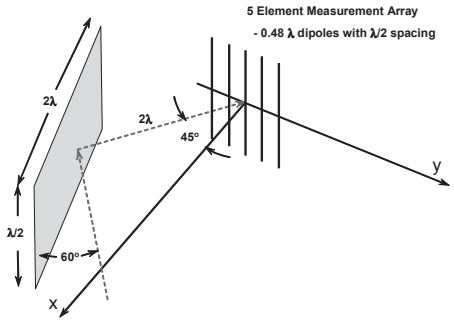

Figure 1: Flat Plate and Measurement Array

For purposes of numerical analysis with NEC4, the surrogate flat plate is synthesized with a collection 41 parallel, half wavelength dipoles oriented in the z direction and packed such that the inter-dipole spacing is 0.05λ. All dipoles have a radius of $8 \cdot 10^{-4}\lambda$. Figure 2 illustrates the locations of the dipoles that synthesize the flat plate and the locations of the probe dipoles used for the NEC4 analysis. In this work, the plane wave excitation for the plate-array configuration will consist conveniently of a z directed electric field with E=1 v/m. The ray paths of the incident and specular scattered field from the plate are shown in Figure 2.

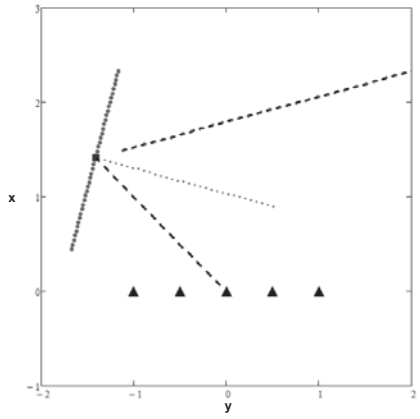

Figure 2: Element locations for NEC4 analysis and paths of incident and specular scattered rays. All dimensions are in wavelengths

Approved for public release; distribution unlimited.

4 Analysis of Flat Plate Current Perturbations Due to the Probe Array

Consider the simulated flat plate and probe array described in previous section. The presence of the probe array perturbs the plane wave induced currents on the plate due to the electromagnetic interaction between the array and the plate. Currents induced in the probe array reradiate to provide an additional illumination source to the plate, thereby causing perturbations from the currents that would be excited otherwise on the plate in free space. These perturbations from the free space, plane wave induced plate currents will cause errors in the measured near field scattering and must be minimized for accurate scattered field measurements. Our strategy for minimizing the array-plate interaction is to cancel the induced currents in the probe array elements. As we shall see, the current cancellation is imperfect for several reasons and our objective is to determine the conditions and degree to which the plate current perturbations can be minimized with this strategy.

4.1 Numerical Analysis of Model Currents

In this section we describe the numerical analysis of the measurement model using NEC4 to account for the electromagnetic interactions between the array and the plate. Specifically, we will evaluate the current distributions on the flat plate under the following three conditions:

1. Flat plate illuminated with a plane wave and no probe array present; this provides the base line current distribution for comparison with the perturbed plate currents induced by the probe array;
2. Flat plate illuminated with a plane wave and the probe array present; here probe array currents are canceled at the element feeds using voltage sources developed with the free space mutual impedances of the probe array;
3. Flat plate illuminated with a plane wave and the probe array present; the probe array currents are canceled at the element feeds using voltage sources developed with the in-situ mutual impedances of the probe array. The in-situ impedances are measured with the probe array in the presence of the flat plate.

To cancel the plane wave induced currents in the probe array, independent voltage sources are applied to each probe array feed point. The sources have the same frequency as the plane wave illumination of the plate-array configuration. The amplitude and phase of each voltage source is set to create a current in the probe array element sufficient to cancel the plane wave induced current in the element. Since there is electromagnetic interaction between the probe array elements, selection of the source amplitude and phase must consider this interaction. In general, the interaction will change due to the presence and orientation of the plate.

For this numerical application, the mutual admittance of the probe array is a convenient characterization of the interaction between the probe array elements. Specifically the currents at

Approved for public release; distribution unlimited.

each probe array feed point, $i_i,\ i = 1, 2, \ldots, 5$, are related to the applied feed voltages, v_i, $i = 1, 2, \ldots, 5$, by the linear admittance matrix as follows:

$$\begin{bmatrix} i_1 \\ i_2 \\ i_3 \\ i_4 \\ i_5 \end{bmatrix} = \begin{bmatrix} y_{11} & y_{12} & y_{13} & y_{14} & y_{15} \\ y_{21} & y_{22} & y_{23} & y_{24} & y_{25} \\ y_{31} & y_{32} & y_{33} & y_{34} & y_{35} \\ y_{41} & y_{42} & y_{43} & y_{44} & y_{45} \\ y_{51} & y_{52} & y_{53} & y_{54} & y_{55} \end{bmatrix} \begin{bmatrix} v_1 \\ v_2 \\ v_3 \\ v_4 \\ v_5 \end{bmatrix},$$

or

$$\bar{I} = \bar{\bar{Y}}\bar{V}.$$

The mutual impedance of the probe array is given by $\bar{\bar{Z}} = \bar{\bar{Y}}^{-1}$.

The mutual admittances and impedances of the probe array can be measured under two conditions. One is when the probe array is located in free space, far from any other object such as the plate. Under these conditions, the probe array admittance will be given by $\bar{\bar{Y}}_{fs}$, where the subscript "fs" denotes free space. The second condition is when the probe array is located in the presence of a scattering body such as the plate. Here the probe array admittance will be given by $\bar{\bar{Y}}_{is}$, where the subscript "is" denotes in-situ. Note that in general, $\bar{\bar{Y}}_{is}$ depends on the location and orientation of the probe array with respect to the scattering body. The corresponding free space and in-situ mutual impedances will be given by $\bar{\bar{Z}}_{fs}$ and $\bar{\bar{Z}}_{is}$ respectively.

For purposes of numerical analysis with NEC4, we compute the short circuit currents at each probe array feed point due to the plane wave excitation and in the presence of the flat plate. We denote these currents by $\bar{I}_p^{pw}$. Here the subscript "p" denotes the presence of the plate and the superscript "pw" denotes the plane wave excitation for the currents. Now the voltages $\bar{V}^c$ at each probe array feed point needed to cancel the currents $\bar{I}_p^{pw}$ are the solution to $-\bar{I}_p^{pw} = \bar{\bar{Y}}\bar{V}^c$ where the minus sign is needed to achieve the current cancellation. The two sets of probe array excitation voltages can be derived as

$$\bar{V}_{fs}^c = -\bar{\bar{Z}}_{fs}\bar{I}_p^{pw}, \tag{1}$$

using the free space mutual impedances and

$$\bar{V}_{is}^c = -\bar{\bar{Z}}_{is}\bar{I}_p^{pw}, \tag{2}$$

using the in-situ mutual impedances.

The probe array admittances can be computed using NEC4 by exciting each probe array feed with a unit voltage source and computing the short circuit currents, $i_i,\ \ i = 1, 2, \ldots, 5$, at each probe array feed. Then $y_{ij} = i_i$ when the unit voltage source is applied to probe feed j. Of course, the probe array admittances are computed with no plane wave excitation of the array-plate structure. Also, the free space admittances are computed when no plate is present and the in-situ admittances are computed with the plate present and oriented with respect to the probe array as it will be when the array currents are to be canceled.

Approved for public release; distribution unlimited.

4.2 Results of the Analysis of the Model Currents

In this section we discuss the results of the numerical analysis of the plate-probe configuration as described in the previous section. We will examine the currents on the dipole elements of the probe array when the currents are canceled using sources developed with the free space admittance matrix and the in-situ admittance matrix. The quality of the cancellation is important for two reasons. First, minimizing the currents on the probe array will minimize the perturbations of the plate currents from those excited by the plane wave alone. Second, the quality of the cancellation influences the accuracy of the open circuit voltage measurements at the probe array feeds. As we shall see in Section 5, these open circuit voltages are important since, when corrected, they are related to the near scattered field to be measured and errors in the open circuit voltages will cause errors in the desired field measurements. This latter point will be investigated in Section 5 of this paper.

In addition, we will examine in this section the perturbations of the currents on the plate due to the presence of the probe array. The baseline for comparison will be the currents induced on the plate in free space when illuminated by a uniform plane wave.

4.2.1 Probe Array Currents

As described earlier, cancellation of the currents on the five elements of the probe array will minimize the perturbations in the currents on the surrogate flat plate from those currents induced by the plane wave alone. Figures 3 and 4 show the effectiveness of cancellation of the probe element currents with active sources at the feed points of each elements.

Figure 3 shows the cancellation when the active source voltages are derived using the mutual impedance matrix for the probe array measured with the array in free space, away from the scattering body. In the Figure we show (a) the currents induced in the elements when the array is in free space and the terminals are short circuited and (b) the currents when the sources derived with the free space mutual impedance matrix are applied at the element terminals. Comparison of these collections of curves indicates that the active loading reduces the current on the dipoles by more than 12 dB at every element. The cancellation is greatest at the central feed point where the free space currents are the greatest.

It is interesting to note that the use of the free space mutual impedances to determine the active source voltages is most effective for those probe array elements at the greatest distance from the plate (i.e. elements 3, 4 and 5). The nearest element (element 1) shows no deep current cancellation due to the active source load at its feed point even though the current in the dipole is reduced by approximately 12 dB when compared to the short circuit currents induced in the free space array. These results are physically consistent with the notion that current cancellation with the free space mutual impedances is most effective for elements away from the target where electromagnetic interactions are likely to be the weakest.

Approved for public release; distribution unlimited.

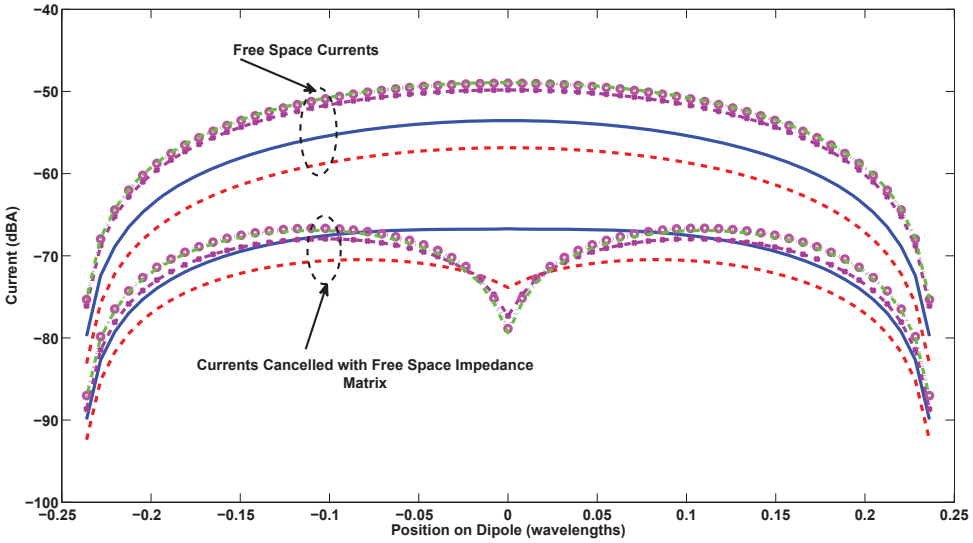

Figure 3: Currents (in dB with respect on one Ampere) along the five elements of the probe array when (a) the array is in free space and the array terminals are short circuited and (b) the array is positioned next to the flat plate and the source voltages derived with the free space mutual impedances of the array are applied to the array terminals. The following is the legend for the curves:

Figure 4 shows similar results when the active source voltages applied to the probe array are determined using the in-situ mutual impedances of the array measured with the probe array oriented with respect to the flat plate as it is when the field measurements are made. Here the active sources are effective in canceling the probe array currents at the load points in all elements of the probe array, including element 1 which is nearest to the plate. In this case the currents are canceled by greater than 15dB in the worst case difference with respect to the free space currents.

4.2.2 Flat Plate Current Perturbations

We have detailed an approach to canceling the dominant mode currents in the probe array elements in an effort to minimize the probe array scattering and its potentially deleterious effect in perturbing target currents. It remains to examine the degree to which this approach is successful by examining the surrogate plate currents in the presence of the probe array with short circuit elements as well as the actively loaded probe array. We consider the active loads as determined using the free space mutual impedances of the probe array as well as the in-situ mutual impedances. As a baseline for comparison, we present the surrogate plate currents in the absence of the probe array.

Approved for public release; distribution unlimited.

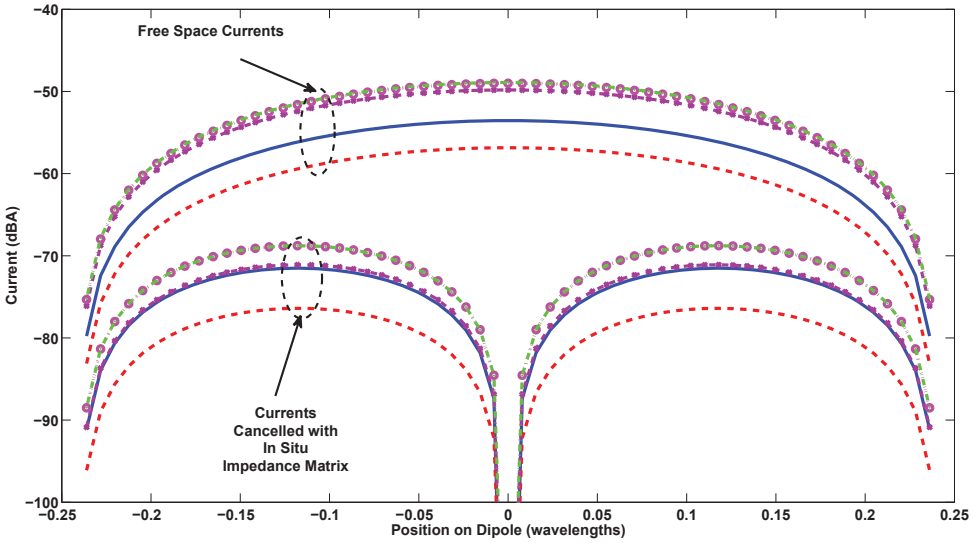

Figure 4: Currents (in dB with respect on one Ampere) along the five elements of the probe array when (a) the array is in free space and the array terminals are short circuited and (b) the array is positioned next to the flat plate and the source voltages derived with the in-situ mutual impedances of the array are applied to the array terminals. The following is the legend for the curves:

Figure 5 shows these plate currents. Figure 5a shows the surrogate plate currents when the plate is in free space without any perturbations due to the probe array. The magnitudes of the plate currents in dB with respect to 1 ampere are shown over the 0.5λ by 2λ surface. The back edge at position 2λ corresponds to the point farthest from the measurement array at point x=2.33λ and y=-1.17λ in Figure 2. For comparison, Figure 5b shows the same currents when the probe array is present and each element of the probe array is short circuited at its feed. point. Perturbations in the plate currents are apparent, especially at a distance of 0.5λ from the plate edge that is near the probe array. Figures 5c and 5d show the plate currents on the surrogate plate when the probe array is present with active loads determined by the free space mutual impedances and the in-situ mutual impedances, respectively. Little perturbations in the plate currents are apparent in these Figures.

Figure 6 shows more quantitatively the perturbations in the plate currents. This Figure shows the plate currents at each dipole center as a function of position along the 2λ extent of the plate. The perturbations in current due to the short circuit probe array are apparent in the solid curve, amounting to almost 3 dBA near the edge closest to the probe array. Little differences (less than 0.5 dBA) occur when the probe array is actively loaded when compared to the baseline currents on the plate in free space.

Approved for public release; distribution unlimited.

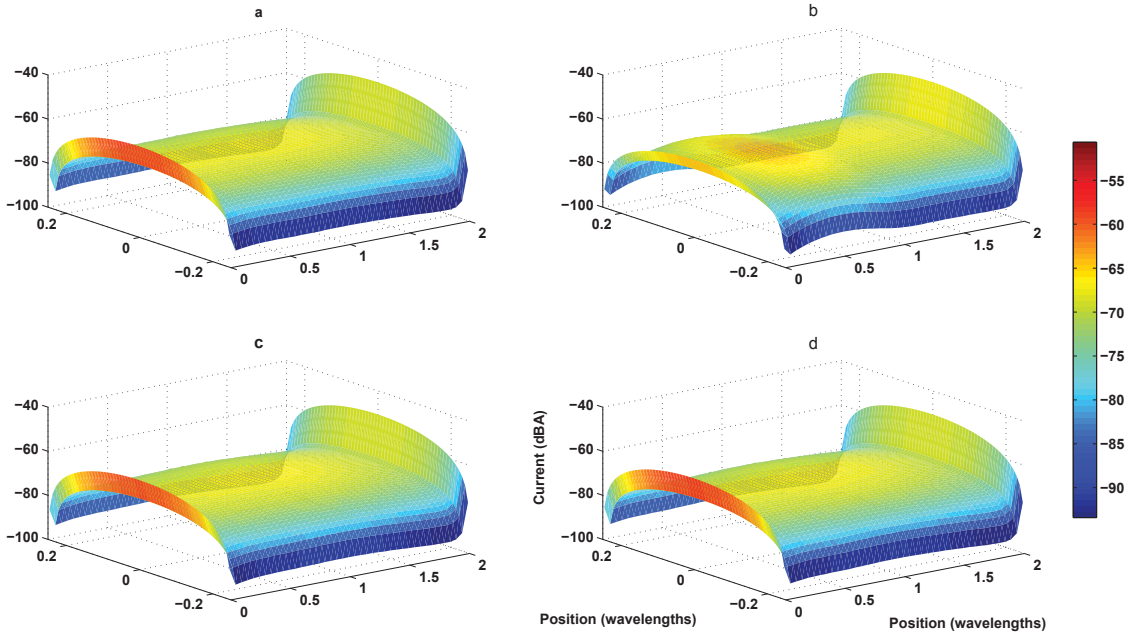

Figure 5: Magnitude of the current on the surrogate flat plate with (a) no probe array present, (b) probe array present with each element short circuited, (c) probe array present with active loading determined by array free space mutual impedances and (d) probe array present with active loading determined by in-situ mutual impedances. Note that the back edge at position 2λ corresponds to the point farthest from the measurement array at point x=2.33λ and y=-1.17λ in Figure 2

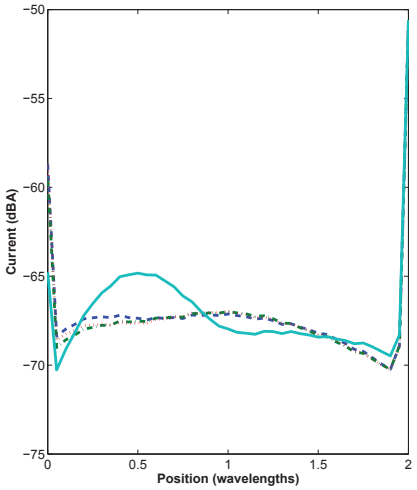

Figure 6: Magnitude of the current on the surrogate flat plate at each dipole center as a function of position along the 2λ dimension of the plate. with (a) short dashed - no probe array present, (b) solid - probe array present with each element short circuited, (c) dot - dash - probe array present with active loading determined by array free space mutual impedances and (d) long dash - probe array present with active loading determined by in-situ mutual impedances. Again, note that the back edge at position 2λ corresponds to the point farthest from the measurement array.

Approved for public release; distribution unlimited.

Based on these observations, it would appear that active loading of the probe array is required to minimize perturbations in the currents on the surrogate plate due to the presence of the array. However, there is little advantage to using in-situ mutual impedances in determining the active loads. This could be a significant advantage in reducing the time required for near field measurements since the probe array mutual impedances need not be measured at each probe array position and orientation with respect to the scattering body. Instead, the probe array mutual impedances need be measured only once when the probe array is in free space and these mutual impedances can be used to determine the active loads on the array for all positions of the array with respect to the scattering body.

These conclusions are preliminary however. In order for the probe array to sample the scattered field accurately, the open circuit voltages at each probe array element must be measured. The probe array currents are canceled imperfectly as illustrated in Figure 3 when the free space mutual impedances of the array are used to determine the active loading necessary to cancel the probe currents. This is especially true for the probe array elements that are nearest to the surrogate flat plate.

In the next section of this report, we will investigate an approach to probe array correction in order to relate the open circuit voltages measured at the probe array elements to the scattered fields on a planar measurement surface. We will evaluate the impact of assuming that the fields that are measured are associated with the target scattering and array radiation in free space. Further, we will determine the errors in the measured open circuit voltages caused by the lack of proper calibration of the probe array.

5 Probe Array Compensation

In this section we relate the open circuit voltages measured at each probe element to the unknown scattered fields from the target. This problem is closely related to that of probe compensated near field measurements for predicting the far-field radiation properties of antennas. This antenna measurement problem has been the subject of extensive research for more than 50 years. Yaghjian [YAG] has provided a comprehensive review of the theory and practice of planar, cylindrical and spherical near-field scanning and processing.

In Section 5.1 we describe a basic analysis of the probe array used for measuring the near zone scattered fields from the target. We use the Lorentz reciprocity theorem to evaluate the surface integral over the scanning plane of the near fields scattered by the target and the near radiated fields from the calibrated probe array in terms of (a) the open circuit voltages measured at the probe array and (b) correction terms involving the reactions of the incident fields with the probe array currents. The reaction terms are evaluated using measurements or calculations of the currents on the elements of the calibrated probe array.

In Sections 5.2 and 5.3 we examine errors implicit in the measurement process. Conventional near field analyses assume that the fields measured and used in the surface integral are those associated with free space conditions when there is no target-array electromagnetic interactions. In Section 5.2 we examine quantitatively the errors associated with this assumption. In Section 5.3 we examine errors due to using realizable active loads on the probe array and imperfect probe array calibration due to the realizable sources used in the calibration process.

Approved for public release; distribution unlimited.

5.1 Basic Analysis

In this work we adapt a theory of near-field antenna measurements with a single probe to the problem of near-field scattering measurements with an array of probes. Specifically, we follow an approach of Paris et. al. [PAR] based on the Lorentz reciprocity theorem [COL, BAL]. The theorem postulates two sets of monochromatic, electromagnetic fields and sources at the same frequency, each satisfying Maxwell's equations and associated boundary conditions. Under quite general conditions, the reciprocity theorem in differential form is

$$\nabla \cdot (\bar{E}_1 \,\mathrm{x}\, \bar{H}_2 - \bar{E}_2 \,\mathrm{x}\, \bar{H}_1) = \bar{E}_2 \cdot \bar{J}_1 - \bar{E}_1 \cdot \bar{J}_2,$$

and, using the divergence theorem, the integral form of the reciprocity theorem is

$$\oint_S (\bar{E}_1 \,\mathrm{x}\, \bar{H}_2 - \bar{E}_2 \,\mathrm{x}\, \bar{H}_1) \cdot \hat{n} dS = \int_V (\bar{E}_2 \cdot \bar{J}_1 - \bar{E}_1 \cdot \bar{J}_2) dV.$$

Here the fields $\bar{E}_1$ and $\bar{H}_1$ result from current sources $\bar{J}_1$ and $\bar{E}_2$ and $\bar{H}_2$ result from current sources $\bar{J}_2$, assuming here that there are no magnetic current sources. In the integral form, the closed surface S encloses the volume V and the unit vector $\hat{n}$ is outward normal to S at each spatial position.

Application of the Lorentz reciprocity theorem to our array near-field measurement problem requires that we first specify the sources and boundary conditions that generate the fields in cases 1 and 2. That is:

Case 1: Here the (flat plate) target and probe array are present and illuminated by the plane wave source. The probe array elements are open circuited at their feed points. See Figure 7. In this analysis, we will be concerned only with the fields scattered by the target and array and not with the incident plane wave. The sources for these scattered fields are then the equivalent currents induced in the plate and probe array elements by the plane wave excitation.

Case 2: Here the (flat plate) target and probe array are present. However, there is no plane wave excitation. Instead, each element of the probe array is driven by a current source at its feed point, providing the sources that are required for the Lorentz reciprocity theorem. See Figure 8.

In this work, we parenthetically include the adjective "flat plate" as a reminder that the results developed here are not restricted to the specific case when the target is a flat plate, as will be studied here.

Approved for public release; distribution unlimited.

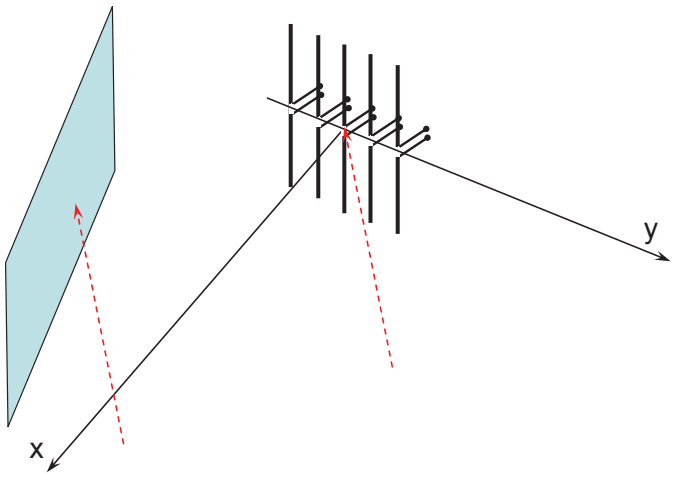

Figure 7: Case 1: Target and probe array illuminated by a plane wave. The probe array elements are open circuited.

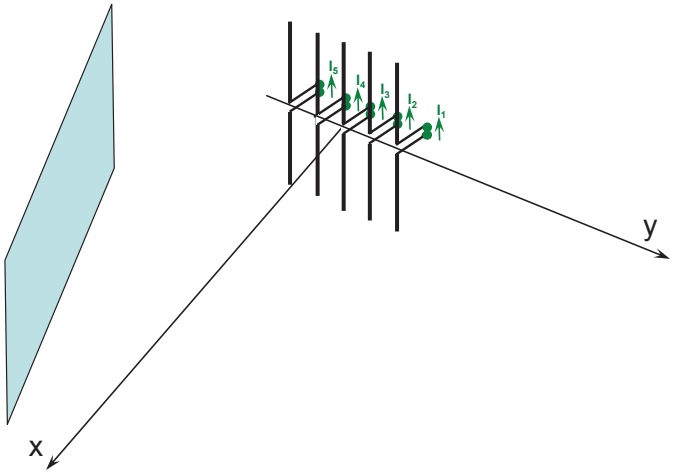

Figure 8: Case 2: Target and probe array with each element of the probe array driven by a current source.

We will employ the integral form of the reciprocity theorem and thus must specify the surface S and associated volume V. Following Paris et. al., the surface will consist of (a) a planar measurement surface, S_m, (b) a spherical surface at a large distance from the target/array ensemble, S_∞, and (c) surfaces just outside the elements of the probe array, S_i, $i = 1, 2, \ldots, I$, where I is the number of probe array elements. These surfaces are shown in Figure 9.

Approved for public release; distribution unlimited.

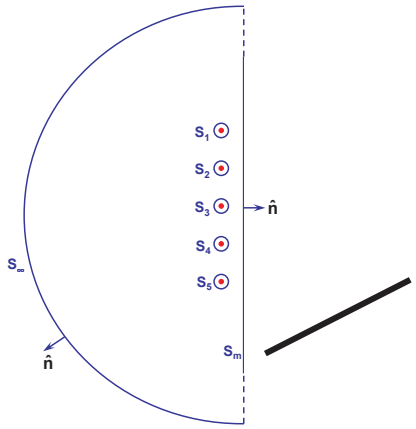

Figure 9: Integration surfaces employed in the Lorentz reciprocity theorem.

The volume enclosed by this surface contains no sources from either case and so the reciprocity theorem becomes

$$\oint_S (\bar{E}_1 \,\mathrm{x}\, \bar{H}_2 - \bar{E}_2 \,\mathrm{x}\, \bar{H}_1) \cdot \hat{n} dS = 0,$$

and we can then write

$$\oint_{S_m} (\bar{E}_1 \,\mathrm{x}\, \bar{H}_2 - \bar{E}_2 \,\mathrm{x}\, \bar{H}_1) \cdot \hat{n} dS + \oint_{S_\infty} (\bar{E}_1 \,\mathrm{x}\, \bar{H}_2 - \bar{E}_2 \,\mathrm{x}\, \bar{H}_1) \cdot \hat{n} dS + \sum_{i=1}^{I} \oint_{S_i} (\bar{E}_{1_i} \,\mathrm{x}\, \bar{H}_{2_i} - \bar{E}_{2_i} \,\mathrm{x}\, \bar{H}_{1_i}) \cdot \hat{n}_i dS = 0. \tag{3}$$

In this expression we first note that

$$\oint_{S_\infty} (\bar{E}_1 \,\mathrm{x}\, \bar{H}_2 - \bar{E}_2 \,\mathrm{x}\, \bar{H}_1) \cdot \hat{n} dS = 0,$$

since at a large distance from the sources, all scattered fields become spherical, transverse EM waves and the integrand vanishes at every point on the distant spherical surface, S_∞ [PAR, page 375]. Then from Equation 3 we find

$$\begin{aligned} \oint_{S_m} (\bar{E}_1 \,\mathrm{x}\, \bar{H}_2 - \bar{E}_2 \,\mathrm{x}\, \bar{H}_1) \cdot \hat{n} dS &= -\sum_{i=1}^{I} \oint_{S_i} (\bar{E}_{1_i} \,\mathrm{x}\, \bar{H}_{2_i} - \bar{E}_{2_i} \,\mathrm{x}\, \bar{H}_{1_i}) \cdot \hat{n}_i dS \\ &= -\sum_{i=1}^{I} \oint_{S_i} (\bar{E}_{1_i} \,\mathrm{x}\, \bar{H}_{2_i} - \bar{E}_{2_i} \,\mathrm{x}\, \bar{H}_{1_i}) \cdot (-\hat{n}_{B_i}) dS \qquad (4) \\ &= \sum_{i=1}^{I} \int_{V_i} (\bar{E}_{2_i} \cdot \bar{J}_{1_i} - \bar{E}_{1_i} \cdot \bar{J}_{2_i}) dV. \end{aligned}$$

Approved for public release; distribution unlimited.

In the second of these equations we have replaced the outward normal vector to the surface S_i, $\hat{n}_i$, by a normal vector $\hat{n}_{B_i}$ perpendicular to the surface of each probe element and pointing outward from the volume occupied by the element. V_i denotes the volume occupied by the i^{th} probe array element. This is illustrated in Figure 10. Finally, we again use the Lorentz reciprocity theorem to express the surface integral in terms of a volume integral involving the fields and sources within each probe element.

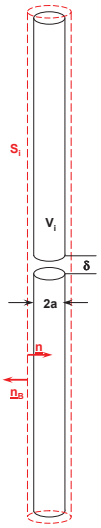

Figure 10: Integration surface around each probe array dipole element.

Consider now the integrand of the element volume integral. We note that for highly conducting elements, $\bar{E}_{2_i} = 0, i = 1, 2 \ldots, I$, everywhere in the element except in the gap that constitutes the element feed. Also, $\bar{J}_{1_i} = 0$, $i = 1, 2 \ldots, I$, in the gap since for case 1 we require that each element of the probe array be open circuited. It follows then that the first term of each element volume integrand vanishes and we can then write

$$\oint_{S_m} (\bar{E}_1 \,\mathrm{x}\, \bar{H}_2 - \bar{E}_2 \,\mathrm{x}\, \bar{H}_1) \cdot \hat{n} dS = -\sum_{i=1}^{I} \int_{V_i} \bar{E}_{1_i} \cdot \bar{J}_{2_i} dV. \tag{5}$$

The volume integral for each element can now be evaluated heuristically. We consider two cases — the gap region and the wire sections of the dipole element. For highly conducting elements, the electric field $\bar{E}_{1_i}$ is the negative of the incident plane wave field in the wire sections, insuring that the total electric field vanishes within the dipole wires. That is

$$\bar{E}_{1_i}(\bar{r}) = -\bar{E}_{inc}(\bar{r}), \;\; \bar{r} \subset V_{wire_i}.$$

Here V_{wire_i} denotes the volume of the wire of the i^{th} probe dipole element.

Approved for public release; distribution unlimited.

Within the the gap, the electric field $\bar{E}_{1_i}$ can be written as

$$\bar{E}_{1_i} = \frac{V^s_{oc_i}}{\delta}\hat{\ell}_i,$$

where $V^s_{oc_i}$ is the open circuit voltage induced in the i^{th} probe element due to the scattering from the target and probe array (case 1) with plane wave excitation, δ is the dimension of the feed gap in the element (see Figure 10)), and $\hat{\ell}_i$ is a unit vector oriented along the i^{th} dipole element. Next, the current density $\bar{J}_{2_i}$ in the gap excited by the current source I_i specified in case 2 can be written as either

$$\bar{J}_{2_i} = \begin{cases} \frac{I_i}{\pi a^2}\hat{\ell}_i & \text{if current uniformly distributed,} \\ \frac{I_i}{2\pi a d_s}\hat{\ell}_i & \text{if current is confined to a skin depth, } d_s. \end{cases}$$

Here a is the radius of the element dipole. In either case, performing the integral over the gap volume V_{gap_i} gives

$$\int_{V_{gap_i}} \bar{E}_{1_i} \cdot \bar{J}_{2_i} dV = V^s_{oc_i} I_i. \tag{6}$$

Then Equation (5) becomes

$$\oint_{S_m} (\bar{E}_1 \,\mathrm{x}\, \bar{H}_2 - \bar{E}_2 \,\mathrm{x}\, \bar{H}_1) \cdot \hat{n} dS = -\sum_{j=1}^{I} V^s_{oc_j} I_j + \sum_{j=1}^{I} \int_{V_{wire_j}} \bar{E}_{inc_j} \cdot \bar{J}_{2_j} dV,$$

where $V_{wire_j} = V_j - V_{gap_j}$. It becomes clear that to measure the open circuit voltage at the i^{th} probe element, for example, $V^s_{oc_i}$, the remaining elements in case 2 must have open circuit terminals so that $I_j = 0, j \neq i$. There results

$$V^s_{oc_i} = -\frac{1}{I_i} \oint_{S_m} (\bar{E}_1 \,\mathrm{x} \bar{H}_{pr_i} - \bar{E}_{pr_i} \,\mathrm{x}\, \bar{H}_1) \cdot \hat{n} dS + \frac{1}{I_i} \sum_{j=1}^{I} \int_{V_{wire_j}} \bar{E}_{inc_j} \cdot \bar{J}_{pr_j} dV, \tag{7}$$

where $\bar{H}_{pr_i} = \bar{H}_2\Big|_{I_j=0,\, j\neq i}$ and $\bar{E}_{pr_i} = \bar{E}_2\Big|_{I_j=0,\, j\neq i}$ are the fields produced by the probe array in the presence of the target when the i^{th} array element is excited by a current source of value I_i and all other elements are open circuited. Also, $\bar{J}_{pr_k} = \bar{J}_{2_k}\Big|_{I_j=0,\, j\neq i}$, $k = 1, 2, \ldots, I$ denotes the current density within the probe element wires in the presence of the target when the i^{th} array element is excited by a current source of value I_i and all other elements are open circuited.

In Appendix 1 we validate Equation (7) by further expanding the surface integral using the reciprocity theorem. However, here we retain the surface integral since, in the conventional theory of near field scanning, the fields in the integrand are expanded in terms of their plane wave spectra in order to relate the far field radiation and scattering properties of the device under test to the measured near field voltages. Note in Equation (7) that the difference between the measured voltage, $V^s_{oc_i}$, and the required surface integral is the superposition of the reactions [RUM] of the incident field on the probe array wire current distributions, $\frac{1}{I_i}\sum_{j=1}^{I} \int_{V_{wire_j}} \bar{E}_{inc_j} \cdot \bar{J}_{pr_j} dV$. Also,

Approved for public release; distribution unlimited.

note that the difference can be written as the sum of the self reaction of the incident field on the measurement dipole wire currents, $\int_{V_{wire_i}} \bar{E}_{inc_i} \cdot \bar{J}_{pr_i} dV$, and the reactions of the incident field on the wire currents in the remaining, open circuit elements of the probe array, $\sum_{j=1,j\neq i}^{I} \int_{V_{wire_j}} \bar{E}_{inc_j} \cdot \bar{J}_{pr_j} dV$. The self reaction is present even for an isolated dipole probe since the current distribution on the dipole is determined largely by the near resonant size of the probe.

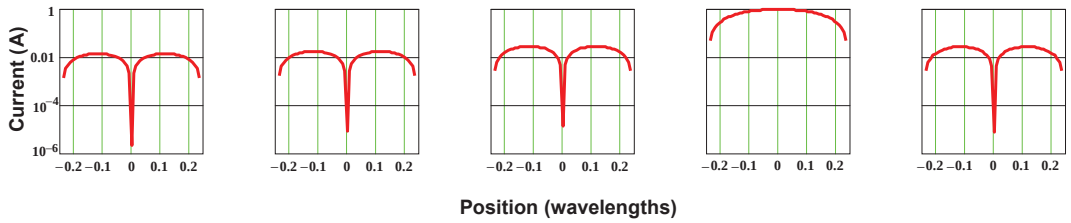

Figure 11: In-situ current distributions on the probe array elements when the fourth element is excited by a unit current source.

Figure 11 shows the in-situ probe array current distributions from NEC4 for case 2 when the fourth array element is excited by a current source of one ampere. The other elements are constrained to have an open circuit at their feeds. Using these current distributions we have found the contributions to the error between the measured voltage and the surface integral due to the measurement (driven) element and the open circuit elements of the array. That is, the error due to self reaction of the driven element, i, is

$$\frac{\left|\int_{V_{wire_i}} \bar{E}_{inc_i} \cdot \bar{J}_{pr_i} dV\right|^2}{\left|\oint_{S_m} (\bar{E}_1 \,\mathrm{x}\bar{H}_{pr_i} - \bar{E}_{pr_i} \,\mathrm{x}\, \bar{H}_1) \cdot \hat{n} dS\right|^2} = 0.84 \; (-0.74\,\mathrm{dB}),$$

and the error due to the open circuit elements is

$$\frac{\left|\sum_{j=1,j\neq i}^{I} \int_{V_{wire_j}} \bar{E}_{inc_j} \cdot \bar{J}_{pr_j} dV\right|^2}{\left|\oint_{S_m} (\bar{E}_1 \,\mathrm{x}\bar{H}_{pr_i} - \bar{E}_{pr_i} \,\mathrm{x}\, \bar{H}_1) \cdot \hat{n} dS\right|^2} = 7.0 \cdot 10^{-3} \; (-21.5\,\mathrm{dB}).$$

In these expression, the surface integral has been evaluated in terms of the probe element currents and the incident field as described further in Appendix 1.

While the error due to the driven element is substantial, it likely differs little from that expected from an isolated dipole since the current distribution on the dipole is determined principally by the near resonant length of the dipole. This error term can be determined numerically from measurements or calculations of the currents on the driven elements. On the other hand, the error due to the open circuit probe elements is small due to the small currents on the elements. Note that these results assume perfect cancellation of the currents on these open circuit elements.

Approved for public release; distribution unlimited.

5.2 Errors Due to the Assumption of No Target-Array Interaction

We turn now to simplifying the first integral in Equation (7) in order to determine the errors in the measured voltage when the fields in the surface integral are assumed to be associated with the probe array and the scatterer when they are individually located in free space. For that purpose, we express the fields for case 1 as

$$\bar{E}_1 = \bar{E}_{1_o} + \delta\bar{E}_1 \tag{8}$$

and

$$\bar{H}_1 = \bar{H}_{1_o} + \delta\bar{H}_1.$$

Here the fields $\bar{E}_{1_o}$ and $\bar{H}_{1_o}$ are the scattered fields from the (flat plate) target when the probe array is absent. These are the fields that we are trying to measure. Then the fields $\delta\bar{E}_1$ and $\delta\bar{H}_1$ represent changes in the fields due to the presence of the open circuited probe array. Each of these scattered fields has a corresponding electric current source distribution. That is, $\bar{J}_1$ distributed over the open circuited probe array and the target is the source for $\bar{E}_1$ and $\bar{J}_{1_o}$distributed over the plate is the source for $\bar{E}_{1_o}$.

In a similar manner for case 2,

$$\bar{E}_{pr_i} = \bar{E}_{pr_{io}} + \delta\bar{E}_{pr_i} \tag{9}$$

and

$$\bar{H}_{pr_i} = \bar{H}_{pr_{io}} + \delta\bar{H}_{pr_i},$$

where the fields $\bar{E}_{pr_{io}}$ and $\bar{H}_{pr_{io}}$ are the radiated fields from the probe array when (a) there is no (flat plate) target present, (b) the i^{th} element is excited and (c) all other elements are open circuited. These are the fields that are conveniently measured to characterize the probe array. Then the fields $\delta\bar{E}_{pr_i}$ and $\delta\bar{H}_{pr_i}$ represent changes in the probe array fields due to the presence of the (flat plate) target. Here too there are electric current sources for the field components. Let $\bar{J}_{pr}$ distributed on the target and elements of the probe array be the source for the field $\bar{E}_{pr_i}$ and $\bar{J}_{pr_o}$distributed on the elements of the probe array be the source for the field $\bar{E}_{pr_{io}}$.

Table 1 summarizes the sources and boundary conditions for each of these fields.

Field	Target	Probe Array	Plane Wave	Probe Array Source	Probe Array Loading
$\bar{E}_1$	Present	Present	Yes	No	Open Circuit (OC)
$\bar{E}_{1_o}$	Present	Absent	Yes	–	–
$\bar{E}_{pr_i}$	Present	Present	No	Yes, element i	All elements except i are OC
$\bar{E}_{pr_{io}}$	Absent	Present	No	Yes, element i	All elements except i are OC

Table 1: Fields, sources and boundary conditions for field expansions.

Approved for public release; distribution unlimited.

With these expansions we find from Equation (7)

$$\begin{aligned} V^s_{oc_i} &= -\tfrac{1}{I_i}\oint_{S_m}((\bar{E}_{1_o}+\delta\bar{E}_1)\,\mathrm{x}(\bar{H}_{pr_{io}}+\delta\bar{H}_{pr_i})-(\bar{E}_{pr_{io}}+\delta\bar{E}_{pr_i})\,\mathrm{x}\,(\bar{H}_{1_o}+\delta\bar{H}_1))\cdot\hat{n}dS \\ &\quad +\tfrac{1}{I_i}\sum_{i=1}^{I}\int_{V_{wire_i}}\bar{E}_{inc_i}\cdot\bar{J}_{pr_i}dV \\ &= -\tfrac{1}{I_i}\oint_{S_m}(\bar{E}_{1_o}\,\mathrm{x}\,\bar{H}_{pr_{io}}-\bar{E}_{pr_{io}}\,\mathrm{x}\,\bar{H}_{1_o})\cdot\hat{n}dS \\ &\quad -\tfrac{1}{I_i}\oint_{S_m}(\bar{E}_{1_o}\,\mathrm{x}\,\delta\bar{H}_{pr_i}-\delta\bar{E}_{pr_i}\,\mathrm{x}\,\bar{H}_{1_o})\cdot\hat{n}dS \\ &\quad -\tfrac{1}{I_i}\oint_{S_m}(\delta\bar{E}_1\,\mathrm{x}\bar{H}_{pr_{io}}-\bar{E}_{pr_{io}}\,\mathrm{x}\,\delta\bar{H}_1)\cdot\hat{n}dS \\ &\quad -\tfrac{1}{I_i}\oint_{S_m}(\delta\bar{E}_1\,\mathrm{x}\,\delta\bar{H}_{pr_i}-\delta\bar{E}_{pr_i}\,\mathrm{x}\,\delta\bar{H}_1)\cdot\hat{n}dS \\ &\quad +\tfrac{1}{I_i}\sum_{j=1}^{I}\int_{V_{wire_j}}\bar{E}_{inc_j}\cdot\bar{J}_{pr_j}dV. \end{aligned} \tag{10}$$

Conventional probe compensation measurements assume no interaction between the probe and antenna or scatterer under test. Thus analysis of the conventional measurements assumes that only the first surface integral, $-\frac{1}{I_i}\oint_{S_m}(\bar{E}_{1_o}\,\mathrm{x}\,\bar{H}_{pr_{io}}-\bar{E}_{pr_{io}}\,\mathrm{x}\,\bar{H}_{1_o})\cdot\hat{n}dS$, needs to be retained. However, since in this work we are interested in the nature of the probe array-target interactions, we will study further the remaining terms in Equation (10).

We apply the Lorentz reciprocity theorem to the second, third and fourth terms in Equation (10). For the second term

$$\begin{aligned} \oint_{S_m}(\bar{E}_{1_o}\,\mathrm{x}\,\delta\bar{H}_{pr_i}-\delta\bar{E}_{pr_i}\,\mathrm{x}\,\bar{H}_{1_o})\cdot\hat{n}dS &= \oint_{S_m+S_\infty}(\bar{E}_{1_o}\,\mathrm{x}\,\delta\bar{H}_{pr_i}-\delta\bar{E}_{pr_i}\,\mathrm{x}\,\bar{H}_{1_o})\cdot\hat{n}dS \\ &= \int_V(\delta\bar{E}_{pr_i}\cdot\bar{J}_{1_o}-\bar{E}_{1_o}\cdot\delta\bar{J}_{pr_i})dV \\ &= -\sum_{j=1}^{I}\int_{V_j}\bar{E}_{1_o}\cdot\delta\bar{J}_{pr_j}dV, \end{aligned}$$

where we have added the vanishing integral over an infinite spherical surface to satisfy the reciprocity theorem and we note that $\bar{J}_{1_o}=\bar{0}$ in the volume V since the probe array is absent in this case. Also, $\delta\bar{J}_{pr_j}$ represents the perturbation in the current density on the j^{th} array element due to introduction of the (flat plate) target.

For the third term

$$\begin{aligned} \oint_{S_m}(\delta\bar{E}_1\,\mathrm{x}\bar{H}_{pr_{io}}-\bar{E}_{pr_{io}}\,\mathrm{x}\,\delta\bar{H}_1)\cdot\hat{n}dS &= \oint_{S_m+S'_\infty}(\delta\bar{E}_1\,\mathrm{x}\bar{H}_{pr_{io}}-\bar{E}_{pr_{io}}\,\mathrm{x}\,\delta\bar{H}_1)\cdot\hat{n}dS \\ &= \int_{V'}(\bar{E}_{pr_{io}}\cdot\delta\bar{J}_1-\delta\bar{E}_1\cdot\bar{J}_{pr_{io}})dV \\ &= \int_{V_{plate}}\bar{E}_{pr_{io}}\cdot\delta\bar{J}_1dV, \end{aligned}$$

Approved for public release; distribution unlimited.

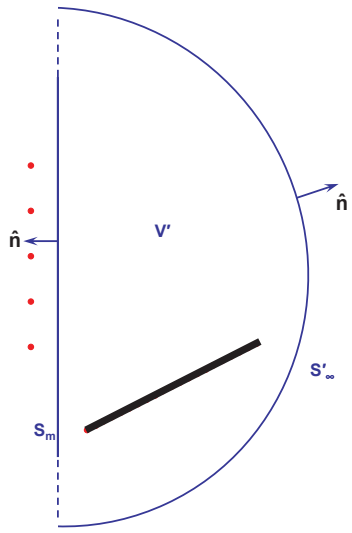

Figure 12: Alternate integration surfaces employed in the Lorentz reciprocity theorem.

where we have added the alternate infinite spherical surface, $S_{\infty}^{'}$, enclosing the plate as shown in Figure 12. Within the volume $V^{'}$ the current $\bar{J}_{pr_{io}} = \bar{0}$ yielding the third line of the equation. Here $\delta\bar{J}_1$ represents the perturbation in the free space plate currents excited by the plane wave when the open circuit probe array is placed near the plate.

An alternate form for the third term results from using the original integration surfaces enclosing the probe array elements. Here we find

$$\begin{aligned}
\oint_{S_m}(\delta\bar{E}_1 \,\mathrm{x}\bar{H}_{pr_{io}} - \bar{E}_{pr_{io}} \,\mathrm{x}\, \delta\bar{H}_1)\cdot\hat{n}dS &= \oint_{S_m+S_\infty}(\delta\bar{E}_1 \,\mathrm{x}\bar{H}_{pr_{io}} - \bar{E}_{pr_{io}} \,\mathrm{x}\, \delta\bar{H}_1)\cdot\hat{n}dS \\
&= \sum_{j=1}^{I}\int_{V_j}(\bar{E}_{pr_{jo}}\cdot\delta\bar{J}_1 - \delta\bar{E}_1\cdot\bar{J}_{pr_{jo}})dV \\
&= -\sum_{j=1}^{I}\int_{V_j}\delta\bar{E}_1\cdot\bar{J}_{pr_{jo}}dV,
\end{aligned}$$

where we have observed that (1) $\bar{E}_{pr_{io}} = \bar{0}$ for each i everywhere within V_i except within the gap, and (2) $\delta\bar{J}_1 = \bar{J}_1 - \bar{J}_{1_o} = \bar{0}$ in the gap since $\bar{J}_1 = \bar{0}$ due to the fact that all probe array elements are open circuited and $\bar{J}_{1_o} = \bar{0}$ due to the fact that the probe array is absent in this case.

Finally, for the fourth term

$$\begin{aligned}
\oint_{S_m}(\delta\bar{E}_1 \,\mathrm{x}\, \delta\bar{H}_{pr_i} - \delta\bar{E}_{pr_i} \,\mathrm{x}\, \delta\bar{H}_1)\cdot\hat{n}dS &= \oint_{S_m+S_\infty}(\delta\bar{E}_1 \,\mathrm{x}\, \delta\bar{H}_{pr_i} - \delta\bar{E}_{pr_i} \,\mathrm{x}\, \delta\bar{H}_1)\cdot\hat{n}dS \\
&= \sum_{j=1}^{I}\int_{V_j}(\delta\bar{E}_{pr_j}\cdot\delta\bar{J}_1 - \delta\bar{E}_1\cdot\delta\bar{J}_{pr_j})dV \\
&= \sum_{j=1}^{I}\int_{V_j}(\bar{E}_{pr_j} - \bar{E}_{pr_{jo}})\cdot(\bar{J}_1 - \bar{J}_{1_o}) \\
&\qquad -(\bar{E}_1 - \bar{E}_{1_o})\cdot(\bar{J}_{pr_j} - \bar{J}_{pr_{jo}})dV \\
&= \sum_{j=1}^{I}\int_{V_j}\bar{E}_{1_o}\cdot\delta\bar{J}_{pr_j}dV,
\end{aligned}$$

Approved for public release; distribution unlimited.

where we have used the field expansions given in Equations (8) and (9) and their related current source equations. The last expression results from consideration of the eight terms in each volume integral as follows:

- $\int_{V_i} \bar{E}_1 \cdot \bar{J}_{pr_i} dV = \left\{ \begin{array}{ll} V_{oc_i}^{pw} I_i & \text{for driven element} \\ 0 & \text{otherwise} \end{array} \right\} - \int_{V_i - V_{gap_i}} \bar{E}_{inc_i} \cdot \bar{J}_{pr_i} dV$; $\bar{E}_1$ is the field scattered by the plate with the array present and all elements are open circuited and so $\bar{E}_1 = -\bar{E}_{inc}(\bar{r})$, $\bar{r} \subset V_{wire_i}$ with $V_{wire_i} = V_i - V_{gap_i}$ for each i . Also, $\bar{J}_{pr_i} = \bar{0}$ in each gap except the driven element. $V_{oc_i}^{pw}$ is the open circuit voltage induced in element i due to plane wave excitation of the plate and open circuit probe array. This portion of the integral is evaluated with the same approach used in the development of Equation (6);

- $\int_{V_i} \bar{E}_1 \cdot \bar{J}_{pr_{i_o}} dV = \left\{ \begin{array}{ll} V_{oc_i}^{pw} I_{o_i} & \text{for driven element} \\ 0 & \text{otherwise} \end{array} \right\} - \int_{V_i - V_{gap_i}} \bar{E}_{inc_i} \cdot \bar{J}_{pr_{i_o}} dV$; Again $\bar{E}_1 = -\bar{E}_{inc}(\bar{r})$, $\bar{r} \subset V_{wire_i}$ for each i except in the gap region and $\bar{J}_{pr_{i_o}} = \bar{0}$ in each gap except the driven element. In this case, I_{o_i}denotes the current source at element i when the probe array is in free space. Again this portion of the integral is evaluated with the same approach used in the development of Equation (6).

  Using these results we find that

$$-\sum_{i=1}^{I} \int_{V_i} \bar{E}_1 \cdot (\bar{J}_{pr_i} - \bar{J}_{pr_{i_o}}) dV = \sum_{i=1}^{I} \int_{V_i - V_{gap_i}} \bar{E}_{inc_i} \cdot (\bar{J}_{pr_i} - \bar{J}_{pr_{i_o}}) dV = \sum_{i=1}^{I} \int_{V_i - V_{gap_i}} \bar{E}_{inc_i} \cdot \delta \bar{J}_{pr_i} dV,$$

  if we assume that $I_{o_i} = I_i$.

- $\int_{V_i} \bar{E}_{1_o} \cdot \bar{J}_{pr_i} dV$ and $\int_{V_i} \bar{E}_{1_o} \cdot \bar{J}_{pr_{i_o}} dV$ must be evaluated directly since neither $\bar{E}_{1_o}$, $\bar{J}_{pr_i}$ nor $\bar{J}_{pr_{i_o}}$ vanish in V_i.

  Again we find

$$\sum_{i=1}^{I} \int_{V_i} \bar{E}_{1_o} \cdot (\bar{J}_{pr_i} - \bar{J}_{pr_{i_o}}) dV = \sum_{i=1}^{I} \int_{V_i} \bar{E}_{1_o} \cdot \delta \bar{J}_{pr_i} dV.$$

- $\int_{V_i} \bar{E}_{pr_i} \cdot \bar{J}_1 dV = 0$; E_{pr_i} is the field excited by the source in the i^{th} probe array element with the plate present and so $\bar{E}_{pr_i} = \bar{0}$ in V_i for all i except in the gap region. Also $\bar{J}_1 = \bar{0}$ in each gap since this is the current in the open circuit array elements with the plate present and a plane wave excitation;

- $\int_{V_i} \bar{E}_{pr_i} \cdot \bar{J}_{1o} dV = 0$; Here $\bar{J}_{1o} = \bar{0}$ in each probe array element since the corresponding field $\bar{E}_{1o}$ is the scattering from the plate with the probe array absent;

- $\int_{V_i} \bar{E}_{pr_{i_o}} \cdot \bar{J}_1 dV = 0$; $\bar{E}_{pr_{i_o}}$is the field excited by the source in the i^{th} probe array element with the plate absent and so $\bar{E}_{pr_{i_o}} = \bar{0}$ in V_i for all i except in the gap region. Also $\bar{J}_1 = \bar{0}$ in each gap since this is the current induced in the open circuit array elements with the plate present and a plane wave excitation; and

- $\int_{V_i} \bar{E}_{pr_{i_o}} \cdot \bar{J}_{1o} dV = 0$; Again $\bar{J}_{1o} = \bar{0}$ in each probe array element since the corresponding field $\bar{E}_{1o}$ is the scattering from the plate with the probe array absent.

Approved for public release; distribution unlimited.

Now from Equation (10) we can write for the observed open circuit voltage at probe terminal i as

$$\begin{aligned}
V^s_{oc_i} &= -\tfrac{1}{I_i}\oint_{S_m}((\bar{E}_{1_o}+\delta\bar{E}_1)\,\mathrm{x}(\bar{H}_{pr_{io}}+\delta\bar{H}_{pr_i})-(\bar{E}_{pr_{io}}+\delta\bar{E}_{pr_i})\,\mathrm{x}\,(\bar{H}_{1_o}+\delta\bar{H}_1))\cdot\hat{n}dS \\
&\quad +\tfrac{1}{I_i}\sum_{j=1}^{I}\int_{V_{wire_j}}\bar{E}_{inc_j}\cdot\bar{J}_{pr_j}dV \\
&= -\tfrac{1}{I_i}\oint_{S_m}(\bar{E}_{1_o}\,\mathrm{x}\,\bar{H}_{pr_{io}}-\bar{E}_{pr_{io}}\,\mathrm{x}\,\bar{H}_{1_o})\cdot\hat{n}dS \\
&\quad +\tfrac{1}{I_i}\sum_{j=1}^{I}\int_{V_j}\bar{E}_{1_o}\cdot\delta\bar{J}_{pr_j}dV \\
&\quad +\tfrac{1}{I_i}\sum_{j=1}^{I}\int_{V_j}\delta\bar{E}_1\cdot\bar{J}_{pr_{jo}}dV \\
&\quad -\tfrac{1}{I_i}\sum_{j=1}^{I}\int_{V_j-V_{gap_j}}\bar{E}_{inc_j}\cdot\delta\bar{J}_{pr_j}dV-\tfrac{1}{I_i}\sum_{j=1}^{I}\int_{V_j}\bar{E}_{1_o}\cdot\delta\bar{J}_{pr_j}dV \\
&\quad +\tfrac{1}{I_i}\sum_{j=1}^{I}\int_{V_{wire_j}}\bar{E}_{inc_j}\cdot\bar{J}_{pr_j}dV \\
&= -\tfrac{1}{I_i}\oint_{S_m}(\bar{E}_{1_o}\,\mathrm{x}\,\bar{H}_{pr_{io}}-\bar{E}_{pr_{io}}\,\mathrm{x}\,\bar{H}_{1_o})\cdot\hat{n}dS \\
&\quad +\tfrac{1}{I_i}\sum_{j=1}^{I}\int_{V_j}\delta\bar{E}_1\cdot\bar{J}_{pr_{jo}}dV+\tfrac{1}{I_i}\sum_{j=1}^{I}\int_{V_{wire_j}}\bar{E}_{inc_j}\cdot\bar{J}_{pr_{jo}}dV,
\end{aligned} \tag{11}$$

since $V_{wire_j}=V_j-V_{gap_j}$.

Again we have assumed that $I_i=I_{o_i}$ or that the current source driving the i^{th} probe array element is the same when the probe array is in free space and when the array is in the presence of the (flat plate) target. In the last equation we have applied the alternate representation for the third term in Equation (10). We verify Equation (11) in the Appendix 2 by expansion of the surface integral and back substitution.

Equation (11) expresses the value of the surface integral in terms of the measured open circuit voltage and correction voltage terms. That is, rewriting Equation (11) we find

$$V^s_{oc_i}=-\frac{1}{I_i}\oint_{S_m}(\bar{E}_{1_o}\,\mathrm{x}\,\bar{H}_{pr_{io}}-\bar{E}_{pr_{io}}\,\mathrm{x}\,\bar{H}_{1_o})\cdot\hat{n}dS+V_\delta+V_{inc_i}+V_{inc}, \tag{12}$$

where the correction terms are

$$\begin{aligned}
V_\delta &= \tfrac{1}{I_i}\sum_{j=1}^{I}\int_{V_j}\delta\bar{E}_1\cdot\bar{J}_{pr_{jo}}dV &&= \text{Voltage induced by perturbed scattered field} \\
V_{inc_i} &= \tfrac{1}{I_i}\int_{V_{wire_i}}\bar{E}_{inc_i}\cdot\bar{J}_{pr_{io}}dV &&= \text{Voltage correction in measurement probe} \\
V_{inc} &= \tfrac{1}{I_i}\sum_{j=1,j\neq i}^{I}\int_{V_{wire_j}}\bar{E}_{inc_j}\cdot\bar{J}_{pr_{jo}}dV &&= \text{Voltage correction due to open circuit probe array elements.}
\end{aligned}$$

It is interesting to observe that the correction voltages are developed as reactions of the perturbed scattered and incident fields with the free space probe array currents with the i^{th} element driven. These currents are shown in Figure 13. They differ little from the in-situ currents shown in Figure 11.

Approved for public release; distribution unlimited.

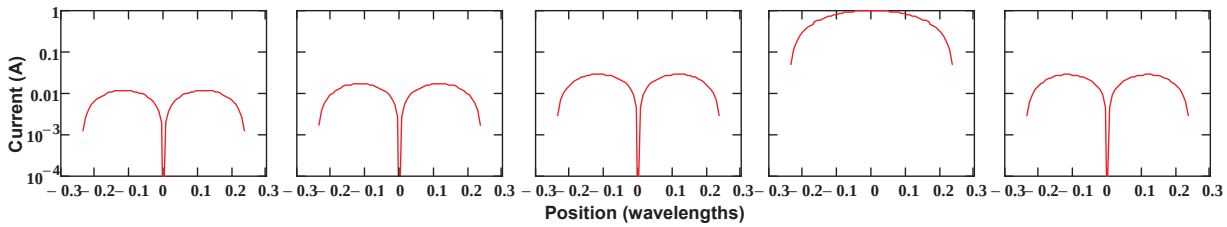

Figure 13: Currents on the elements of a five element probe array with the array in free space (no target present); the fourth array element is excited by a unit current source and the remaining element are open circuited.

The correction voltage V_δ due to perturbations in the scattered field due to the presence of the probe array is generally unknown since the field perturbations are unknown. Thus, this correction voltage cannot be applied to the measured voltage and must be minimized. Alternatively, the correction voltages V_{inc_i} and V_{inc} are known from measurements of the free space incident field and measurements or computations of the free space current distributions on the probe array elements. These correction voltages may be used to correct the measured open circuit voltage, $V^s_{oc_i}$, to obtain a more accurate sample of the desired surface integral in Equation (12).

It is interesting to observe the relative magnitudes of these correction voltages for the problem described earlier where the scattering from a surrogate flat plate is observed with the fourth element of a five element probe array. The NEC4 numerical analysis of this problem provides the following:

$$\frac{\left|V_\delta\right|^2}{\left|\frac{1}{I_i}\oint_{S_m}(\bar{E}_1 \,\mathrm{x}\bar{H}_{pr_i} - \bar{E}_{pr_i}\,\mathrm{x}\,\bar{H}_1)\cdot\hat{n}dS\right|^2} = \frac{\left|\frac{1}{I_i}\sum_{j=1}^{I}\int_{V_j}\delta\bar{E}_1\cdot\bar{J}_{pr_{jo}}dV\right|^2}{\left|\frac{1}{I_i}\oint_{S_m}(\bar{E}_1 \,\mathrm{x}\bar{H}_{pr_i} - \bar{E}_{pr_i}\,\mathrm{x}\,\bar{H}_1)\cdot\hat{n}dS\right|^2} = 8.4{\cdot}10^{-4}\ (-31\mathrm{dB}),$$

$$\frac{\left|V_{inc_i}\right|^2}{\left|\frac{1}{I_i}\oint_{S_m}(\bar{E}_1 \,\mathrm{x}\bar{H}_{pr_i} - \bar{E}_{pr_i}\,\mathrm{x}\,\bar{H}_1)\cdot\hat{n}dS\right|^2} = \frac{\left|\frac{1}{I_i}\int_{V_{wire_i}}\bar{E}_{inc_i}\cdot\bar{J}_{pr_{io}}dV\right|^2}{\left|\frac{1}{I_i}\oint_{S_m}(\bar{E}_1 \,\mathrm{x}\bar{H}_{pr_i} - \bar{E}_{pr_i}\,\mathrm{x}\,\bar{H}_1)\cdot\hat{n}dS\right|^2} = 6.8\ (8.3\,\mathrm{dB}),\ \text{and}$$

$$\frac{\left|V_{inc}\right|^2}{\left|\frac{1}{I_i}\oint_{S_m}(\bar{E}_1 \,\mathrm{x}\bar{H}_{pr_i} - \bar{E}_{pr_i}\,\mathrm{x}\,\bar{H}_1)\cdot\hat{n}dS\right|^2} = \frac{\left|\frac{1}{I_i}\sum_{j=1,j\neq i}^{I}\int_{V_{wire_j}}\bar{E}_{inc_j}\cdot\bar{J}_{pr_{jo}}dV\right|^2}{\left|\frac{1}{I_i}\oint_{S_m}(\bar{E}_1 \,\mathrm{x}\bar{H}_{pr_i} - \bar{E}_{pr_i}\,\mathrm{x}\,\bar{H}_1)\cdot\hat{n}dS\right|^2} = 0.05\ (-12.7\,\mathrm{dB}).$$

These numerical results indicate that

(a) the correction voltage, V_δ, due to perturbation of the scattered field by the probe array is small. Recall that this voltage us unknown and so cannot be used as a correction to the measured voltage. Thus, it is required that this voltage be small so that it can be neglected;

Approved for public release; distribution unlimited.

(b) the correction voltage, V_{inc_i}, due to the reaction of the incident field on the wire currents of the measurement element of the probe array is significant and must be used to correct the measured voltage much as it would be if the element were in free space; and

(c) the correction voltage, V_{inc}, due to the reaction of the incident field on the wire elements of the canceled elements of the probe array is small because of the canceled currents; potentially it is possible to apply these correction voltages to the measured voltage.

This study of probe array compensation indicates that it is important to minimize the perturbation in the scattered field due to the presence of the probe array since the perturbations induce an error in the measured voltage in the probe array which cannot be corrected. However, results of this admittedly small numerical study indicate that this perturbation error voltage is small. This is in agreement with the results of Section 4.2.2 where we found little advantage in the use of the in-situ mutual impedances to design the cancellation of the currents in the probe array. Further, in this development of probe array compensation, we find that using the currents designed with free space mutual impedances is required as the basis for determining correction voltages to be applied to the probe array measurements.

5.3 Errors Due to the Measurement Process

The preceeding analysis assumes that probe array currents are perfectly canceled for purposes of measuring the open circuit voltages representative of the integral of the near zone scattered field. Perfect cancellation is difficult to achieve experimentally and the lack of perfect cancellation will introduce additional errors in the measurements. In this section we analyze the imperfect cancellation problem by introducing active loads at the probe array terminals with the objective of estimating these additional errors under realistic conditions.

We return to the development in Section 5.1 where we defined the fields and sources for each case required in the Lorentz reciprocity theorem. Here case 1 is revised such that the surrogate plate and probe array are illuminated by a plane wave and the probe array elements have active loads characterized by Thévenin equivalent circuits. The parameters of the i^{th} Thévenin equivalent circuit are its open circuit voltage, V_{T_i}, and equivalent series impedance, Z_{T_i}. This case is illustrated in Figure 14 and is called Case 1a.

Similarly, case 2 is revised with the flat plate target excited by the probe array with each element of the array driven by a Norton equivalent source. The parameters of the Norton equivalent circuit at the i^{th} probe array terminal are the current source with value I_{N_i} and shunt admittance Y_{N_i}. This is Case 2a and is shown in Figure 15.

Here our analysis of probe compensation with the Lorentz reciprocity theorem begins with Equation (4) given by

$$\oint_{S_m} (\bar{E}_1 \,\mathrm{x}\, \bar{H}_2 - \bar{E}_2 \,\mathrm{x}\, \bar{H}_1) \cdot \hat{n} dS = \sum_{i=1}^{I} \int_{V_i} (\bar{E}_{2_i} \cdot \bar{J}_{1_i} - \bar{E}_{1_i} \cdot \bar{J}_{2_i}) dV.$$

Approved for public release; distribution unlimited.

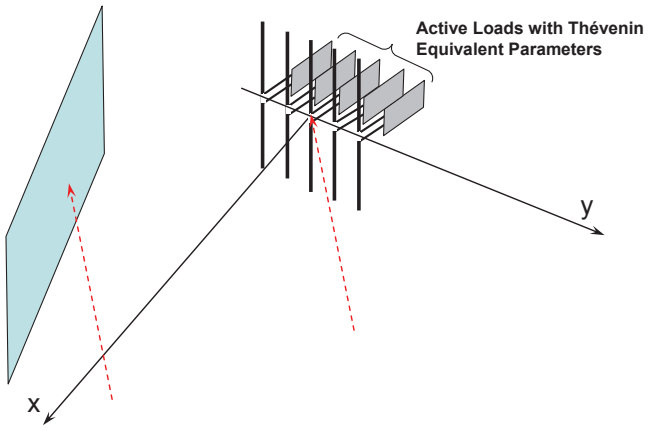

Figure 14: Case 1a: Target and probe array illuminated by a plane wave. The probe array elements are loaded with Thévenin equivalent circuits.

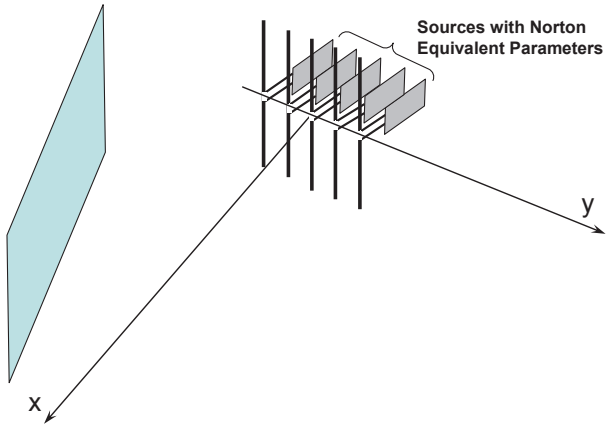

Figure 15: Case 2a: Target and probe array with each element of the probe array driven by a Norton equivalent source.

In this case, we find that $\bar{E}_{2_i}(\bar{r}) = \bar{0}$, when $\bar{r} \subset V_{wire_i}$and $\bar{E}_{1_i}(\bar{r}) = -\bar{E}_{inc}(\bar{r})$, when $\bar{r} \subset V_{wire_i}$. Substituting these results gives

$$\oint_{S_m} (\bar{E}_1 \,\mathrm{x}\, \bar{H}_2 - \bar{E}_2 \,\mathrm{x}\, \bar{H}_1) \cdot \hat{n} dS = \sum_{i=1}^{I} \int_{V_{gap_i}} (\bar{E}_{2_i} \cdot \bar{J}_{1_i} - \bar{E}_{1_i} \cdot \bar{J}_{2_i}) dV + \sum_{j=1}^{I} \int_{V_{wire_j}} \bar{E}_{inc_j} \cdot \bar{J}_{2_j} dV. \quad (13)$$

This result is similar to that which we developed in the basic analysis of Section 5.1. There we evaluated the reaction terms, $\sum_{j=1}^{I} \int_{V_{wire_j}} \bar{E}_{inc_j} \cdot \bar{J}_{2_j} dV$, and found that only the self reaction on the measurement element of the probe array was significant and the sum of the reactions on the open circuit elements was relatively small. These terms can be found by computation based on measurements of the incident electric field and the measurements or calculations of the currents on the probe array dipole elements.

We focus now on the integrals involving the fields and currents in the gap region. As we saw in

Approved for public release; distribution unlimited.

Section 5.1 we can express the electric field in the gap region as

$$\bar{E}_{\alpha_i} = \frac{V_{\alpha_i}}{\delta}\hat{\ell}_i,$$

and the current density in the gap can be modeled as

$$\bar{J}_{\beta_i} = \begin{cases} \frac{I_{\beta_i}}{\pi a^2}\hat{\ell}_i & \text{if current uniformly distributed,} \\ \frac{I_{\beta_i}}{2\pi a d_s}\hat{\ell}_i & \text{if current is confined to a skin depth, } d_s. \end{cases}$$

The parameters δ and a are as defined in Figure 10 and represent the dimension of the dipole gap and the radius of the dipole, respectively. Also, α and β denote the case for application of the Lorentz reciprocity theorem. It follows that

$$\int_{V_{gap_i}} \bar{E}_{\alpha_i} \cdot \bar{J}_{\beta_i} dV = V_{\alpha_i} I_{\beta_i},$$

and

$$\sum_{i=1}^{I} \int_{V_{gap_i}} (\bar{E}_{2_i} \cdot \bar{J}_{1_i} - \bar{E}_{1_i} \cdot \bar{J}_{2_i}) dV = \overline{V}_2^T \overline{I}_1 - \overline{V}_1^T \overline{I}_2, \tag{14}$$

where the voltage and current column matrices are given by

$$\begin{aligned} \overline{V}_1 &= [V_{1_1} V_{1_2} \dots V_{1_I}]^T \\ \overline{V}_2 &= [V_{2_1} V_{2_2} \dots V_{2_I}]^T \\ \overline{I}_1 &= [I_{1_1} I_{1_2} \dots I_{1_I}]^T \\ \overline{I}_2 &= [I_{2_1} I_{2_2} \dots I_{2_I}]^T. \end{aligned}$$

The notation $[\cdot]^T$ denotes matrix transpose.

For case 2a, the voltages V_{2_i} can be found from the in-situ mutual admittance matrix for the probe array and the Norton equivalent sources at each probe array terminal. For the probe array, the in-situ admittance matrix relates the currents and voltages at each terminal as

$$\begin{bmatrix} i_1 \\ i_2 \\ i_3 \\ i_4 \\ i_5 \end{bmatrix} = \begin{bmatrix} y_{11} & y_{12} & y_{13} & y_{14} & y_{15} \\ y_{21} & y_{22} & y_{23} & y_{24} & y_{25} \\ y_{31} & y_{32} & y_{33} & y_{34} & y_{35} \\ y_{41} & y_{42} & y_{43} & y_{44} & y_{45} \\ y_{51} & y_{52} & y_{53} & y_{54} & y_{55} \end{bmatrix} \begin{bmatrix} v_1 \\ v_2 \\ v_3 \\ v_4 \\ v_5 \end{bmatrix},$$

or

$$\overline{I}_2 = \overline{\overline{Y}}_{is} \overline{V}_2, \tag{15}$$

where the in-situ admittance matrix of the probe array is given by

$$\overline{\overline{Y}}_{is} = \begin{bmatrix} y_{11} & y_{12} & y_{13} & y_{14} & y_{15} \\ y_{21} & y_{22} & y_{23} & y_{24} & y_{25} \\ y_{31} & y_{32} & y_{33} & y_{34} & y_{35} \\ y_{41} & y_{42} & y_{43} & y_{44} & y_{45} \\ y_{51} & y_{52} & y_{53} & y_{54} & y_{55} \end{bmatrix}.$$

Approved for public release; distribution unlimited.

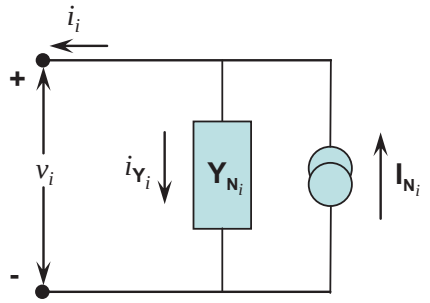

Figure 16: Norton equivalent circuit for probe array terminal i.

The Norton equivalent circuit at terminal i is shown in Figure 16. It follows from this circuit that

$$i_i = I_{N_i} - Y_{N_i} v_i,$$

or

$$\overline{I}_2 = \overline{I}_N - \overline{\overline{Y}}_N \overline{V}_2.$$

Here the Norton admittance matrix is given by

$$\overline{\overline{Y}}_N = \begin{bmatrix} Y_{N_1} & 0 & 0 & 0 & 0 \\ 0 & Y_{N_2} & 0 & 0 & 0 \\ 0 & 0 & Y_{N_3} & 0 & 0 \\ 0 & 0 & 0 & Y_{N_4} & 0 \\ 0 & 0 & 0 & 0 & Y_{N_5} \end{bmatrix},$$

and $\overline{I}_N = [I_{N_1} I_{N_2} \ldots I_{N_I}]^T$.

Applying this to Equation (15) gives

$$\overline{I}_N = \left[\overline{\overline{Y}}_{is} + \overline{\overline{Y}}_N\right] \overline{V}_2,$$

where we have equated the terminal voltages to those required in Equation (14), i.e. $v_{i,} \equiv V_{2_i}$ $i = 1, 2, \ldots, 5$. Thus we can solve for $\overline{V}_2$ as

$$\overline{V}_2 = \left[\overline{\overline{Y}}_{is} + \overline{\overline{Y}}_N\right]^{-1} \overline{I}_N. \tag{16}$$

From Figure 16, the current $I_{2_i} \equiv i_i = I_{N_i} - Y_{N_i} V_{2_i}$. Then

$$\overline{I}_2 = \overline{I}_N - \overline{\overline{Y}}_N \overline{V}_2. \tag{17}$$

Turning now to Case 1a, we consider the Thévenin equivalent circuit shown in Figure 17 at each terminal of the probe array.

Approved for public release; distribution unlimited.

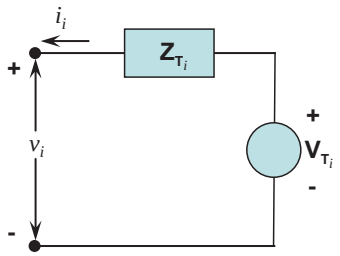

Figure 17: Thévenin equivalent circuit for probe array teminal i.

Previously [SCH, Equation (3)] we found that the plane wave excited probe array could be characterized as

$$\begin{bmatrix} v_1 \\ v_2 \\ v_3 \\ v_4 \\ v_5 \end{bmatrix} = \begin{bmatrix} V_{P_1} \\ V_{P_2} \\ V_{P_3} \\ V_{P_4} \\ V_{P_5} \end{bmatrix} + \begin{bmatrix} z_{11} & z_{12} & z_{13} & z_{14} & z_{15} \\ z_{21} & z_{22} & z_{23} & z_{24} & z_{25} \\ z_{31} & z_{32} & z_{33} & z_{34} & z_{35} \\ z_{41} & z_{42} & z_{43} & z_{44} & z_{45} \\ z_{51} & z_{52} & z_{53} & z_{54} & z_{55} \end{bmatrix} \begin{bmatrix} i_1 \\ i_2 \\ i_3 \\ i_4 \\ i_5 \end{bmatrix},$$

or

$$\overline{V}_1 = \overline{V}_P + \overline{\overline{Z}}_{is}\overline{I}_1, \tag{18}$$

where the voltages V_{P_i} are the open circuit voltages at the probe array terminals excited by the plane wave with the (flat plate) target present and $\overline{V}_P = [V_{P_1} V_{P_2} \dots V_{P_5}]^T$. The impedance matrix, $\overline{\overline{Z}}_{is} = \overline{\overline{Y}}_{is}^{-1}$, with elements $z_{i,j}$, is the in-situ impedance matrix characterizing the array in the presence of the (flat plate) target. With the Thévenin load at each terminal we find that

$$v_i = V_{T_i} - Z_{T_i} i_i,$$

or

$$\overline{V}_1 = \overline{V}_T - \overline{\overline{Z}}_T \overline{I}_1, \tag{19}$$

where

$$\overline{\overline{Z}}_T = \begin{bmatrix} Z_{T_1} & 0 & 0 & 0 & 0 \\ 0 & Z_{T_2} & 0 & 0 & 0 \\ 0 & 0 & Z_{T_3} & 0 & 0 \\ 0 & 0 & 0 & Z_{T_4} & 0 \\ 0 & 0 & 0 & 0 & Z_{T_5} \end{bmatrix},$$

and $\overline{V}_T = [V_{T_1} V_{T_2} \dots V_{T_5}]^T$.

Approved for public release; distribution unlimited.

Applying this to Equation (18) gives

$$\begin{bmatrix} V_{T_1} - V_{P_1} \\ V_{T_2} - V_{P_2} \\ V_{T_3} - V_{P_3} \\ V_{T_4} - V_{P_4} \\ V_{T_5} - V_{P_5} \end{bmatrix} = \begin{bmatrix} z_{11} + Z_{T_1} & z_{12} & z_{13} & z_{14} & z_{15} \\ z_{21} & z_{22} + Z_{T_2} & z_{23} & z_{24} & z_{25} \\ z_{31} & z_{32} & z_{33} + Z_{T_3} & z_{34} & z_{35} \\ z_{41} & z_{42} & z_{43} & z_{44} + Z_{T_4} & z_{45} \\ z_{51} & z_{52} & z_{53} & z_{54} & z_{55} + Z_{T_5} \end{bmatrix} \overline{I}_1.$$

This enables us to find the terminal currents $i_i \equiv I_{1_i}\ i = 1, 2, \ldots, 5$, which are required in Equation (14). That is

$$\overline{I}_1 = \left[\overline{\overline{Z}}_{is} + \overline{\overline{Z}}_T\right]^{-1} \left[\overline{V}_T - \overline{V}_P\right]. \tag{20}$$

We can find the probe array terminal voltages for this case from the Thévenin equivalent circuit using Equations (19) and (20).

Using Equations (16) and (17) for case 2a we find for the gap integrals in Equation (14)

$$\begin{aligned} \sum_{i=1}^{I} \int_{V_{gap_i}} (\bar{E}_{2_i} \cdot \bar{J}_{1_i} - \bar{E}_{1_i} \cdot \bar{J}_{2_i}) dV &= \overline{V}_2^T \overline{I}_1 - \overline{V}_1^T \overline{I}_2 \\ &= \overline{I}_N^T \left[\overline{\overline{Y}}_{is} + \overline{\overline{Y}}_N\right]^{-1} \overline{I}_1 - \overline{V}_1^T (\overline{I}_N - \overline{\overline{Y}}_N \overline{V}_2) \\ &= \overline{I}_N^T \left[\overline{\overline{Y}}_{is} + \overline{\overline{Y}}_N\right]^{-1} \overline{I}_1 - \overline{V}_1^T (\overline{I}_N - \overline{\overline{Y}}_N \left[\overline{\overline{Y}}_{is} + \overline{\overline{Y}}_N\right]^{-1} \overline{I}_N) \\ &= \overline{I}_N^T \left\{ \left[\overline{\overline{Y}}_{is} + \overline{\overline{Y}}_N\right]^{-1} \overline{I}_1 - \overline{V}_1 + \left[\overline{\overline{Y}}_{is} + \overline{\overline{Y}}_N\right]^{-1} \overline{\overline{Y}}_N \overline{V}_1 \right\} \\ &= \overline{I}_N^T \left\{ \left[\overline{\overline{Y}}_{is} + \overline{\overline{Y}}_N\right]^{-1} \overline{I}_1 - (\overline{\overline{I}} - \left[\overline{\overline{Y}}_{is} + \overline{\overline{Y}}_N\right]^{-1} \overline{\overline{Y}}_N) \overline{V}_1 \right\}. \end{aligned}$$

Now we examine the case 1a relations given by Equations (18) and (20) to find

$$\begin{aligned} \sum_{i=1}^{I} \int_{V_{gap_i}} (\bar{E}_{2_i} \cdot \bar{J}_{1_i} - \bar{E}_{1_i} \cdot \bar{J}_{2_i}) dV &= \overline{I}_N^T \left\{ \left[\overline{\overline{Y}}_{is} + \overline{\overline{Y}}_N\right]^{-1} \overline{I}_1 - (\overline{\overline{I}} - \left[\overline{\overline{Y}}_{is} + \overline{\overline{Y}}_N\right]^{-1} \overline{\overline{Y}}_N)(\overline{V}_P + \overline{\overline{Z}}_{is} \overline{I}_1) \right\} \\ &= -\overline{I}_N^T (\overline{\overline{I}} - \left[\overline{\overline{Y}}_{is} + \overline{\overline{Y}}_N\right]^{-1} \overline{\overline{Y}}_N) \overline{V}_P \\ &\quad + \overline{I}_N^T \left\{ \left[\overline{\overline{Y}}_{is} + \overline{\overline{Y}}_N\right]^{-1} - (\overline{\overline{I}} - \left[\overline{\overline{Y}}_{is} + \overline{\overline{Y}}_N\right]^{-1} \overline{\overline{Y}}_N) \overline{\overline{Z}}_{is} \right\} \overline{I}_1 \\ &= -\overline{I}_N^T (\overline{\overline{I}} - \left[\overline{\overline{Y}}_{is} + \overline{\overline{Y}}_N\right]^{-1} \overline{\overline{Y}}_N) \overline{V}_P \\ &\quad + \overline{I}_N^T \left\{ \left[\overline{\overline{Y}}_{is} + \overline{\overline{Y}}_N\right]^{-1} - (\overline{\overline{I}} - \left[\overline{\overline{Y}}_{is} + \overline{\overline{Y}}_N\right]^{-1} \overline{\overline{Y}}_N) \overline{\overline{Z}}_{is} \right\} \\ &\quad \cdot \left[\overline{\overline{Z}}_{is} + \overline{\overline{Z}}_T\right]^{-1} \left[\overline{V}_T - \overline{V}_P\right] \\ &= V_c, \end{aligned}$$

where

$$V_c = -\overline{I}_N^T (\overline{\overline{I}} - \left[\overline{\overline{Y}}_{is} + \overline{\overline{Y}}_N\right]^{-1} \overline{\overline{Y}}_N) \overline{V}_P.$$

This follows from consideration of the factor in braces in the second and third terms3 given by

$$\overline{\overline{B}} \equiv \left[\overline{\overline{Y}}_{is} + \overline{\overline{Y}}_N\right]^{-1} - (\overline{\overline{I}} - \left[\overline{\overline{Y}}_{is} + \overline{\overline{Y}}_N\right]^{-1} \overline{\overline{Y}}_N) \overline{\overline{Z}}_{is} = \overline{\overline{0}}.$$

Approved for public release; distribution unlimited.

The fact that $\overline{\overline{B}}$ vanishes follows from the following development:

$$\begin{aligned}\left[\overline{\overline{Y}}_{is}+\overline{\overline{Y}}_{N}\right]\overline{\overline{B}} &= \overline{\overline{I}}-(\left[\overline{\overline{Y}}_{is}+\overline{\overline{Y}}_{N}\right]-\overline{\overline{Y}}_{N})\overline{\overline{Z}}_{is}\\ &= \overline{\overline{I}}-\overline{\overline{Y}}_{is}\overline{\overline{Z}}_{is}\\ &= \overline{\overline{0}} \text{ and it follows that}\\ \overline{\overline{B}} &= \overline{\overline{0}} \text{ when } \left[\overline{\overline{Y}}_{is}+\overline{\overline{Y}}_{N}\right]\neq\overline{\overline{0}}.\end{aligned}$$

Note the special case when $\overline{\overline{Y}}_{N}=\overline{\overline{0}}$ gives

$$\sum_{i=1}^{I}\int_{V_{gap_i}}(\bar{E}_{2_i}\cdot\bar{J}_{1_i}-\bar{E}_{1_i}\cdot\bar{J}_{2_i})dV=V_c=-\overline{I}_{N}^{T}\overline{V}_{P}.$$

As we have seen previously in this special case, setting the i^{th} current source in case 2a to 1 Ampere (i.e. $I_{N_I}=1\text{Amp}$) and the remaining current sources to zero, gives $-\overline{I}_{N}^{T}\overline{V}_{P}=-V_{P_i}$, the required plane wave induced open circuit voltage at probe array port i.

Returning to the general case with active Thévenin loads and Norton sources, we require that the case 2a current sources be such that only one probe array element has unit terminal currents. In this case

$$\overline{I}_2=\widehat{I}_i=\overline{I}_N-\overline{\overline{Y}}_{N}\overline{V}_2=\overline{I}_N-\overline{\overline{Y}}_{N}\left[\overline{\overline{Y}}_{is}+\overline{\overline{Y}}_{N}\right]^{-1}\overline{I}_N=(\overline{\overline{I}}-\overline{\overline{Y}}_{N}\left[\overline{\overline{Y}}_{is}+\overline{\overline{Y}}_{N}\right]^{-1})\overline{I}_N, \tag{21}$$

where $\widehat{I}_i=[0_1,0_2,\ldots 1_i,\ldots,0_I]^T$ is a unit vector on the i^{th} probe array dimension. Then the Norton equivalent sources must be

$$\overline{I}_N=(\overline{\overline{I}}-\overline{\overline{Y}}_{N}\left[\overline{\overline{Y}}_{is}+\overline{\overline{Y}}_{N}\right]^{-1})^{-1}\widehat{I}_i$$

and the response due to the correctly calibrated probe array becomes

$$\begin{aligned}V_c &= -\overline{I}_{N}^{T}(\overline{\overline{I}}-\left[\overline{\overline{Y}}_{is}+\overline{\overline{Y}}_{N}\right]^{-1}\overline{\overline{Y}}_{N})\overline{V}_{P}\\ &= -\widehat{I}_{i}^{T}(\overline{\overline{I}}-\left[\overline{\overline{Y}}_{is}+\overline{\overline{Y}}_{N}\right]^{-1}\overline{\overline{Y}}_{N})^{-T}(\overline{\overline{I}}-\left[\overline{\overline{Y}}_{is}+\overline{\overline{Y}}_{N}\right]^{-1}\overline{\overline{Y}}_{N})\overline{V}_{P}\\ &= -\widehat{I}_{i}^{T}\overline{V}_{P}=-V_{P_i}.\end{aligned}$$

In this expression $[\cdot]^{-T}$ denotes the transpose of the matrix inverse. Since the admittance matrices are symmetric, we will keep in mind that the transpose of the inverse is equal to the matrix inverse. Thus, we find from this expression that when the probe array is calibrated in-situ, the measured voltage is the plane wave induced voltage at the i^{th} terminal of the probe array.

However, we have observed that it is far more efficient to calibrate the probe array when it is in free space, away from the target to be measured. Here only one set of mutual admittances for the probe array must be measured and used to calibrate the probe array for every position and orientation of the array with respect to the target. Using the free space admittances of the array, $\overline{\overline{Y}}_{fs}$, the current sources must be

$$\overline{I}_{N}^{fs}=(\overline{\overline{I}}-\overline{\overline{Y}}_{N}\left[\overline{\overline{Y}}_{fs}+\overline{\overline{Y}}_{N}\right]^{-1})^{-1}\widehat{I}_i,$$

Approved for public release; distribution unlimited.

where we have assumed that the Norton terminal admittances for the free space probe array are the same as those for the in-situ array. Here the response due to the free space calibrated probe array is

$$V_c^{fs} = -\widehat{I}_i^T(\overline{\overline{I}} - \left[\overline{\overline{Y}}_{fs} + \overline{\overline{Y}}_N\right]^{-1}\overline{\overline{Y}}_N)^{-T}(\overline{\overline{I}} - \left[\overline{\overline{Y}}_{is} + \overline{\overline{Y}}_N\right]^{-1}\overline{\overline{Y}}_N)\overline{V}_P. \tag{22}$$

Note that when the probe array is calibrated with high impedance sources ($\overline{\overline{Y}}_N = \overline{\overline{0}}$) then $V_c^{fs} = -\widehat{I}_i^T\overline{V}_P = -V_{P_i}$ independent of whether the array is calibrated in free space or in the presence of the probe array.

It is interesting to compare the probe array element open circuit voltages when the array is calibrated in free space with the voltages when the array is calibrated with the in-situ admittances. Here we will compare the difference between these voltages with the required surface integral in a quantity given by

$$10\log\left[\frac{\left|V_c^{fs} - V_c\right|^2}{\left|\frac{1}{I_i}\oint_{S_m}(\bar{E}_1 \,\mathrm{x}\bar{H}_{pr_i} - \bar{E}_{pr_i}\,\mathrm{x}\,\bar{H}_1)\cdot\hat{n}dS\right|^2}\right] \text{ (dB)}.$$

For the sample problem consisting of the surrogate flate plate and a five element probe array considered here, this measure of calibration error varies from -12.5 dB for the array element closest to the plate to -17.9 dB for the element farthest from the plate. For these results we have assumed that the Norton admittance at each element is matched to the free space admittance of the probe array element. That is, $Y_{N_i} = y_{i,i}^*$ where $y_{i,i}^*$ is the complex conjugate of the admittance of the i^{th} array element when the array is located in free space with no target present.

These results indicate that when the probe array elements are close to the test target, errors increase in the measured open circuit voltages as a measure of the surface integral. The element closest to the flat plate target introduces an error of -12.5 dB and that closest element is located within 3/4 wavelength from the edge of the plate. See Figure 2. Also, the element farthest from the plate is approximately 2 3/4 wavelengths from the plate and introduces an error of -17.9 dB. Thus it appears from this limited numerical study that in-situ calibration of the probe array may be necessary when elements of the probe array come within two wavelengths of the target.

Experimentally it is difficult to calibrate the probe array such that the terminal currents are perfectly canceled. To investigate the error in the measured voltage V_c due to imperfect cancellation of the terminal currents we return to Equation (21) with

$$\overline{I}_2 = \widehat{I}_i + \overline{E} = (\overline{\overline{I}} - \overline{\overline{Y}}_N\left[\overline{\overline{Y}}_{is} + \overline{\overline{Y}}_N\right]^{-1})\overline{I}_N,$$

where $\overline{E} = [e_1, e_2, \ldots e_i, \ldots, e_I]^T$ represents the residual error or noise at each array terminal when the probe array is experimentally calibrated. It follows that the Norton equivalent sources with noise are

$$\overline{I}_N = (\overline{\overline{I}} - \overline{\overline{Y}}_N\left[\overline{\overline{Y}}_{is} + \overline{\overline{Y}}_N\right]^{-1})^{-1}(\widehat{I}_i + \overline{E})$$

Approved for public release; distribution unlimited.

and the errored response due to the correctly calibrated probe array becomes

$$\begin{aligned} V_{ce} &= -\overline{I}_N^T(\overline{\overline{I}} - \left[\overline{\overline{Y}}_{is} + \overline{\overline{Y}}_N\right]^{-1}\overline{\overline{Y}}_N)\overline{V}_P \\ &= -(\widehat{I}_i^T + \overline{E}^T)(\overline{\overline{I}} - \left[\overline{\overline{Y}}_{is} + \overline{\overline{Y}}_N\right]^{-1}\overline{\overline{Y}}_N)^{-T}(\overline{\overline{I}} - \left[\overline{\overline{Y}}_{is} + \overline{\overline{Y}}_N\right]^{-1}\overline{\overline{Y}}_N)\overline{V}_P \\ &= -V_{P_i} - \overline{E}^T\overline{V}_P \\ &= V_c - \overline{E}^T\overline{V}_P. \end{aligned}$$

The error or noise power in the measurement of V_c is given by

$$\begin{aligned} N_c &= \mathscr{E}\left\{\left|\overline{E}^T\overline{V}_P\right|^2\right\} \\ &= \mathscr{E}\left\{\sum_{i=1}^{I}\sum_{j=1}^{I} e_i V_{P_i} e_j^* V_{P_j}^*\right\} \\ &= \sum_{i=1}^{I}\sum_{j=1}^{I} V_{P_i} V_{P_j}^* \mathscr{E}\left\{e_i e_j^*\right\} \\ &= \sum_{i=1}^{I}\sum_{j=1}^{I} V_{P_i} V_{P_j}^* E_o \delta_{i,j} \\ &= E_o|V_P|^2, \end{aligned}$$

where $\mathscr{E}\{\cdot\}$ denotes the ensemble average with respect to the random error or noise samples and we have assumed that the residual noise samples at each array terminal are independent with zero mean and common variance given by E_o.

With these results we can find the signal to error noise ratio of the in-situ calibrated probe array output as among

$$SNR_{cn} = \frac{|V_{P_i}|^2}{N_c} = \frac{|V_{P_i}|^2}{E_o|V_P|^2} = SNR_i. \tag{23}$$

Here $SNR_i = 1/E_o$ denotes the signal to noise of the probe array terminal currents, assuming that the measurement dipole is calibrated with a one Ampere source and the last result follows from the fact that $|V_P|^2 = |V_{P_i}|^2$ when the probe array is calibrated with the target present.

Equation (23) indicates that the signal to error noise ratio of the measured open circuit voltage equals the signal to error noise of the calibration current in the measurement element of the probe array when the array is calibrated in-situ.

In the case when the probe array is calibrated with free space admittances, we find that the Norton equivalent current sources are

$$\overline{I}_N = (\overline{\overline{I}} - \overline{\overline{Y}}_N\left[\overline{\overline{Y}}_{fs} + \overline{\overline{Y}}_N\right]^{-1})^{-1}(\widehat{I}_i + \overline{E}),$$

and

$$\begin{aligned} V_{cn} &= -\overline{I}_N^T(\overline{\overline{I}} - \left[\overline{\overline{Y}}_{is} + \overline{\overline{Y}}_N\right]^{-1}\overline{\overline{Y}}_N)\overline{V}_P \\ &= -(\widehat{I}_i^T + \overline{E}^T)(\overline{\overline{I}} - \left[\overline{\overline{Y}}_{fs} + \overline{\overline{Y}}_N\right]^{-1}\overline{\overline{Y}}_N)^{-T}(\overline{\overline{I}} - \left[\overline{\overline{Y}}_{is} + \overline{\overline{Y}}_N\right]^{-1}\overline{\overline{Y}}_N)\overline{V}_P \\ &= V_c^{fs} + \overline{E}^T(\overline{\overline{I}} - \left[\overline{\overline{Y}}_{fs} + \overline{\overline{Y}}_N\right]^{-1}\overline{\overline{Y}}_N)^{-T}(\overline{\overline{I}} - \left[\overline{\overline{Y}}_{is} + \overline{\overline{Y}}_N\right]^{-1}\overline{\overline{Y}}_N)\overline{V}_P. \end{aligned}$$

Approved for public release; distribution unlimited.

In this case, the signal to error noise of the free space calibrated probe array is

$$\begin{aligned} SNR_{cn} &= \frac{\left|V_{P_i}\right|^2}{E_o\left|(\bar{\bar{I}}-\left[\overline{\overline{Y}}_{fs}+\overline{\overline{Y}}_N\right]^{-1}\overline{\overline{Y}}_N)^{-T}(\bar{\bar{I}}-\left[\overline{\overline{Y}}_{is}+\overline{\overline{Y}}_N\right]^{-1}\overline{\overline{Y}}_N)\overline{V}_P\right|^2} \\ &= SNR_i\frac{\left|V_{P_i}\right|^2}{\left|(\bar{\bar{I}}-\left[\overline{\overline{Y}}_{fs}+\overline{\overline{Y}}_N\right]^{-1}\overline{\overline{Y}}_N)^{-T}(\bar{\bar{I}}-\left[\overline{\overline{Y}}_{is}+\overline{\overline{Y}}_N\right]^{-1}\overline{\overline{Y}}_N)\overline{V}_P\right|^2}. \end{aligned} \tag{24}$$

Thus the signal to error noise of the measured open circuit voltage is degraded when the probe array is calibrated in free space. This SNR degradation is given by the factor

$$\delta_{SNR_{cn}} = \frac{\left|V_{P_i}\right|^2}{\left|(\bar{\bar{I}}-\left[\overline{\overline{Y}}_{fs}+\overline{\overline{Y}}_N\right]^{-1}\overline{\overline{Y}}_N)^{-T}(\bar{\bar{I}}-\left[\overline{\overline{Y}}_{is}+\overline{\overline{Y}}_N\right]^{-1}\overline{\overline{Y}}_N)\overline{V}_P\right|^2}.$$

For the problem described earlier consising of the surrogate flat plate and the five element probe array, this signal to error noise degradation varies from -5.3 dB to -13.1 dB among the probe elements. Thus it appears that there can be significant degradation in the accuracy with which the open circuit voltages are measured when there is failure to achieve open circuit conditions in the array elements due to free space calibration of the probe array.

6 Conclusions and Recommendations

In this work we analyzed technical problems associated with the use of an array of probes to measure simultaneously the near fields scattered by a target. The measurements are made with the objective of estimating the far zone bistatic scattering from the target using established electromagnetic signal processing techniques. An array of probes is proposed for the purpose of speeding the collection of required near field samples. However, the array increases the potential for electromagnetic coupling between the array and the target, thereby distorting the fields to be measured. Further, mutual coupling between array elements in the presence of the scattering body may change the near field measured at each probe array element when compared to that measured by an isolated probe.

To minimize the array-target coupling, we proposed that the array employ active loading at each array element to minimize currents on the array elements. Proper active loading requires knowledge of the mutual impedances between array elements, which, in general, depend on the location and orientation of the array with respect to the scattering target. To assess the requirement for measurements of in-situ mutual impedances, we considered a probe array with strong interaction between the target and the array. Specifically we considered a surrogate flat plate with a five element dipole probe array located near the plate and in the direction of the specular, plane wave induced scattering from the plate. We investigated the perturbations on the plane wave induced currents on the plate due to the presence of the loaded, five element dipole

Approved for public release; distribution unlimited.

probe array. Numerical results using NEC4 indicated that active loading of the probe array is required to minimize the perturbations in the target currents. However, we found in this case that there is little advantage to using in-situ mutual impedances in determining the active loads. If this result is generalized, it could be significant in reducing the time required for near field measurements since the probe array mutual impedances need not be measured at each probe array position and orientation with respect to the scattering body. Instead, the probe array mutual impedances need to be measured only once when the probe array is in free space and these mutual impedances can be used to determine the active loads on the array for all positions of the array with respect to the scattering body.

However, this is not the complete story. The coupling between the array and the target under test can introduce errors in the measured voltages at the probe array elements. These errors are due to (a) the assumption that there is no target-array coupling in interpreting the measurements, (b) calibration of the probe array in free space where there is no interaction with the target and (c) failure to achieve adequate current cancellation in the probe array elements during measurements of the open circuit voltages at the array elements. To address these additional sources of error, we provided a probe array compensation theory based on the Lorentz reciprocity theorem. The theory permits expression of the open circuit probe array voltages in terms of (a) the required surface integral involving the near fields scattered by the target and the near fields radiated by the probe array with no target-array interaction and (b) correction voltages due to the presence of the array elements and the target-array interactions. The correction voltages are of two types. One type is due to perturbations in the target scattered field because of the presence of the probe array. This correction voltage is unknown and not available for compensation of the measured voltage at the probe array. Another type of correction voltage is associated with plane wave induced currents on the probe array when located in free space. These correction voltages can be developed as part of the probe array calibration and measurements of the incident plane wave. A numerical study of the surrogate flat plate-probe array configuration indicated that (a) corrections to the measured probe array voltages due to perturbations in the scattered field from the presence of the probe array are small, even when cancellation of the probe array currents is determined using the free space mutual impedances of the array, and (b) corrections due to the presence of the other elements of the probe array can be important but the corrections can be determined in terms of the free space current distributions on the array as part of the array calibration process.

In addition, errors in the probe array voltage measurements are introduced by the use of realizable sources in the probe array during calibration and realizable loads during scattering measurements. When the array is calibrated in free space and used to cancel the array currents during near field measurements, errors in the open circuit voltages as large as -12.5 dB were observed for the plate-array problem analyzed here. These measurement errors are most signficant for the array elements that are close to the target under test. Experimental errors in achieving probe array current cancellation cause errors in the voltage measurements as well. In fact, these errors are increased due to calibration of the probe array in free space by as much as 13 dB for the plate-array problem considered here.

These conclusions are potentially significant since they seem to indicate that free space mutual impedances of the probe array are sufficient for the simultaneous measurement of near scattered field samples with small error so long as elements of the array are not too close to the target

Approved for public release; distribution unlimited.

under test. The effective use of free space mutual impedances obviates the need for in-situ impedance measurements at each location and orientation of the probe array with respect to the scattering body which would slow the overall measurement process. It would seem that a hybrid measurement process should be considered. For probe array locations and orientations with respect to the target when there is likely to be large coupling, in-situ mutual impedances would be required, slowing the measurement process. When little coupling is anticipated, the free space mutual impedances of the array can be used, thereby speeding the measurement process.

However, these conclusions are based on a limited numerical investigation of one probe array structure and target configuration. This suggests further study of (a) the precision with which probe array current cancellation is experimentally achievable, (b) additional configurations of dipole probe arrays with respect to a larger selection of scattering targets, and (b) other elements for the probe array such as aperture or microstrip elements as might be used in practical measurement arrays.

7 Acknowledgments

The support for this work from the Air Force Office of Scientific Research is gratefully acknowledged. I appreciate the technical discussions with Dr. Kris Kim and Dr. Hans Steyskal that were important in developing the ideas described here. Ms Terry O'Donnell provided important software to interface NEC4 with MATLAB and I appreciate her generous commitment of time to assist in modifying this software.

8 Appendices

8.1 Appendix 1 - Verification of Equation (7)

Here we validate Equation (7) which gives the open circuited scattered voltage. Equation (7) is

$$V^s_{oc_i} = -\frac{1}{I_i}\oint_{S_m}(\bar{E}_1 \,\mathrm{x}\bar{H}_{pr_i} - \bar{E}_{pr_i}\,\mathrm{x}\,\bar{H}_1)\cdot\hat{n}dS + \frac{1}{I_i}\sum_{j=1}^{I}\int_{V_{wire_j}}\bar{E}_{inc_j}\cdot\bar{J}_{pr_j}dV.$$

Using the reciprocity theorem to expand the surface integral we find

$$\begin{aligned}
\oint_{S_m}(\bar{E}_1 \,\mathrm{x}\bar{H}_{pr_i} - \bar{E}_{pr_i}\,\mathrm{x}\,\bar{H}_1)\cdot\hat{n}dS &= \oint_{S_m+S_\infty}(\bar{E}_1 \,\mathrm{x}\bar{H}_{pr_i} - \bar{E}_{pr_i}\,\mathrm{x}\,\bar{H}_1)\cdot\hat{n}dS \\
&= \sum_{j=1}^{I}\int_{V_j}(\bar{E}_{pr_j}\cdot\bar{J}_1 - \bar{E}_1\cdot\bar{J}_{pr_j})dV \\
&= \sum_{j=1}^{I}\int_{V_{gap_j}}\bar{E}_{pr_j}\cdot\bar{J}_1 dV - \sum_{j=1}^{I}\int_{V_{wire_j}}\bar{E}_1\cdot\bar{J}_{pr_j}dV - \int_{V_{gap_i}}\bar{E}_1\cdot\bar{J}_{pr_i}dV \\
&= -\sum_{j=1}^{I}\int_{V_{wire_j}}\bar{E}_1\cdot\bar{J}_{pr_j}dV - \int_{V_{gap_i}}\bar{E}_1\cdot\bar{J}_{pr_i}dV.
\end{aligned}$$

In the third line we have noted that $\bar{E}_{pr_j}(\bar{r}) = \bar{0},\ \bar{r} \subset\ V_{wire_j}\ j = 1, 2, \ldots, I.$ and $\bar{J}_{pr_j}(\bar{r}) = \bar{0},\ \bar{r}\ \subset V_{gap_j}\ \forall\, j \neq i$. Also, in the fourth line we have used $\bar{J}_1(\bar{r}) = \bar{0},\ \bar{r}\ \subset\ V_{gap_j},\ j = 1, 2, \ldots, I.$ Then we can write, using the fact that $\bar{E}_1(\bar{r}) + \bar{E}_{inc}(\bar{r}) = \bar{0},\ \bar{r}\ \subset\ V_{wire}$, that

$$\begin{aligned}
V^s_{oc_i} &= \tfrac{1}{I_i}\sum_{j=1}^{I}\textstyle\int_{V_{wire_j}}\bar{E}_1\cdot\bar{J}_{pr_j}dV + \tfrac{1}{I_i}\int_{V_{gap_i}}\bar{E}_1\cdot\bar{J}_{pr_i}dV + \tfrac{1}{I_i}\sum_{j=1}^{I}\int_{V_{wire_j}}\bar{E}_{inc_j}\cdot\bar{J}_{pr_j}dV \\
&= \tfrac{1}{I_i}\textstyle\int_{V_{gap_i}}\bar{E}_1\cdot\bar{J}_{pr_i}dV,
\end{aligned}$$

which validates the development.

Approved for public release; distribution unlimited.

8.2 Appendix 2 - Verification of Equation (11)

In this appendix, we confirm the result given in Equation (11) by expansion of the surface integral using the Lorentz reciprocity theorem. From Equation (11)

$$\begin{aligned}
V^s_{oc_i} &= -\tfrac{1}{I_i}\oint_{S_m}(\bar{E}_{1_o}\,\mathrm{x}\,\bar{H}_{pr_{io}} - \bar{E}_{pr_{io}}\,\mathrm{x}\,\bar{H}_{1_o})\cdot\hat{n}dS \\
&\quad +\tfrac{1}{I_i}\sum_{j=1}^{I}\int_{V_j}\delta\bar{E}_1\cdot\bar{J}_{pr_{jo}}dV + \tfrac{1}{I_i}\sum_{j=1}^{I}\int_{V_{wire_j}}\bar{E}_{inc_j}\cdot\bar{J}_{pr_{jo}}dV \\
&= -\tfrac{1}{I_i}\sum_{j=1}^{I}\int_{V_j}(\bar{E}_{pr_{jo}}\cdot\bar{J}_{1_o} - \bar{E}_{1_o}\cdot\bar{J}_{pr_{jo}})dV \\
&\quad +\tfrac{1}{I_i}\sum_{j=1}^{I}\int_{V_j}\delta\bar{E}_1\cdot\bar{J}_{pr_{jo}}dV + \tfrac{1}{I_i}\sum_{j=1}^{I}\int_{V_{wire_j}}\bar{E}_{inc_j}\cdot\bar{J}_{pr_{jo}}dV \\
&= \tfrac{1}{I_i}\sum_{j=1}^{I}\int_{V_j}\bar{E}_{1_o}\cdot\bar{J}_{pr_{jo}}dV \\
&\quad +\tfrac{1}{I_i}\sum_{j=1}^{I}\int_{V_j}\delta\bar{E}_1\cdot\bar{J}_{pr_{jo}}dV + \tfrac{1}{I_i}\sum_{j=1}^{I}\int_{V_{wire_j}}\bar{E}_{inc_j}\cdot\bar{J}_{pr_{jo}}dV \\
&= \tfrac{1}{I_i}\sum_{j=1}^{I}\int_{V_j}\bar{E}_1\cdot\bar{J}_{pr_{jo}}dV + \tfrac{1}{I_i}\sum_{j=1}^{I}\int_{V_{wire_j}}\bar{E}_{inc_j}\cdot\bar{J}_{pr_{jo}}dV \\
&= \tfrac{1}{I_i}\sum_{j=1}^{I}\int_{V_{gap_j}}\bar{E}_1\cdot\bar{J}_{pr_{jo}}dV \\
&= \tfrac{1}{I_i}\int_{V_{gap_i}}\bar{E}_1\cdot\bar{J}_{pr_{io}}dV \\
&= V^s_{oc_i},
\end{aligned}$$

since we have assumed that $I_i = I_{i_o}$.

Approved for public release; distribution unlimited.

9 References

[BAL] Balanis, Constantine A., Advanced Engineering Electromagnetics, John Wiley and Sons, 1989, ISBN 0-471-62194-3, pp 323-328.

[COL] Collin, R. E. and F. J. Zucker, Antenna Theory (Part 1), McGraw Hill Book Company, 1969, pp 24-25.

[PAR] Paris, D. T., W. M. Leach, Jr. and E. B. Joy, "Basic Theory of Probe-Compensated Near-Field Measurements," IEEE Transactions on Antennas and Propagation, AP-26, No. 3. May 1978, pp 373-379.

[RUM] Rumsey, V. H., "Reaction Concept in Electromagnetic Theory," Physical Review, 94, 1954, pp 1483-1491.

[SCH] Schindler, J. K., "An Approach to Minimizing Probe Array/Target Interactions for Near Field Scattering Measurements," AFRL Technical Report, AFRL-RY-HS-TR-2011-00781, May 2011.

[YAG] Yaghjian, Arthur, D., "An Overview of Near-Field Antenna Measurements," IEEE Transactions on Antennas and Propagation, AP-34, No. 1, January 1986, pp 30-45.

Approved for public release; distribution unlimited.